END

MICROCOPY RESOLUTION TEST CHART

NATIONAL BUREAU OF STANDARDS-1963-A

ELECTRICAL TRANSPORT IN SILICA
THERMALLY GROWN ON SILICON

Final Report for the Period
1 February 1982 through 31 August 1984

By

J. Bruce Wagner, Jr.

November 20, 1984

To

U.S. Army Research Office

Contract DAAG 29-82-K-0052

Center for Solid State Science
Arizona State University
Tempe, AZ 85287

AD-A150 304

DTIC FILE COPY

DTIC
ELECTE
FEB 1 2 1985

E

85   01   29   140

REPORT DOCUMENTATION PAGE	READ INSTRUCTIONS BEFORE COMPLETING FORM

1. REPORT NUMBER ARO 17888.3-MS	2. GOVT ACCESSION NO. AD-A150 304	3. RECIPIENT'S CATALOG NUMBER N/A

4. TITLE *(and Subtitle)* Transport Properties of Silica Thermally Grown on Silicon	5. TYPE OF REPORT & PERIOD COVERED Final Report 2/1/82 – 8/31/84
	6. PERFORMING ORG. REPORT NUMBER

7. AUTHOR(s) J. Bruce Wagner, Jr.	8. CONTRACT OR GRANT NUMBER(s) DAAG 29-82-K-0052

9. PERFORMING ORGANIZATION NAME AND ADDRESS	10. PROGRAM ELEMENT, PROJECT, TASK AREA & WORK UNIT NUMBERS

11. CONTROLLING OFFICE NAME AND ADDRESS U. S. Army Research Office Post Office Box 12211 Research Triangle Park, NC 27709	12. REPORT DATE November 20, 1984
	13. NUMBER OF PAGES 70

14. MONITORING AGENCY NAME & ADDRESS(*if different from Controlling Office*)	15. SECURITY CLASS. *(of this report)* Unclassified
	15a. DECLASSIFICATION/DOWNGRADING SCHEDULE

16. DISTRIBUTION STATEMENT *(of this Report)*

Approved for public release; distribution unlimited.

17. DISTRIBUTION STATEMENT *(of the abstract entered in Block 20, if different from Report)*

NA

18. SUPPLEMENTARY NOTES

The view, opinions, and/or findings contained in this report are those of the author(s) and should not be construed as an official Department of the Army position, policy, or decision, unless so designated by other documentation.

19. KEY WORDS *(Continue on reverse side if necessary and identify by block number)*

Electrical Conductivity, Transport/Transference Numbers, Silica, Quartz Crystals

20. ABSTRACT *(Continue on reverse side if necessary and identify by block number)*

The total, ionic and electronic conductivity of silica thermally grown on silicon have been determined between 25° – 960°C. Therefrom the ionic transport numbers have been calculated. Utilizing an open circuit emf method, the average ionic transport numbers for silica thermally grown on silicon, for vitreous silica and for single crystalline quartz have been determined between 550 and 950°C.

In general, all the silicas studied exhibit mixed conduction, i.e., conduction via ions and

DD FORM 1473 EDITION OF 1 NOV 65 IS OBSOLETE

electrons. The ionic contribution increases with temperature and attains a maximum at $800° - 900°C$. The open circuit emf studies show smaller values of the average ionic transference numbers than those values obtained via conductivity measurements. This apparent discrepancy is attributed to migration of oxygen through pores in the SiO_2 grown on Si in the case of the open circuit emf measurement. High resolution transmission electron microscopic studies confirmed the presence of small pores (5 to 8 $\overset{\circ}{A}$ in diameter) in the SiO_2 grown on silicon under both wet and dry conditions.

A preliminary study of the reaction between molybdenum and SiO_2 grown thermally on silicon wafers has been carried out. Mo appears to diffuse into the SiO_2 at 1000°C and 1100°C as determined by Rutherford Back Scattering techniques. Further studies are in progress. Originator furnished keywords includ..

SCIENTIFIC PERSONNEL
SUPPORTED BY CONTRACT DAAG 29-82-K-0052

Dr. Jitendra K. Srivastava   1 September 1982 – 31 August 1984
Faculty Research Associate

Mr. Ashok Khandkar   1 May 1983 – 30 June 1983
Graduate Student

Prof. J. B. Wagner, Jr.   1 month Summer 1983
Principal Investigator   2 weeks Summer 1984
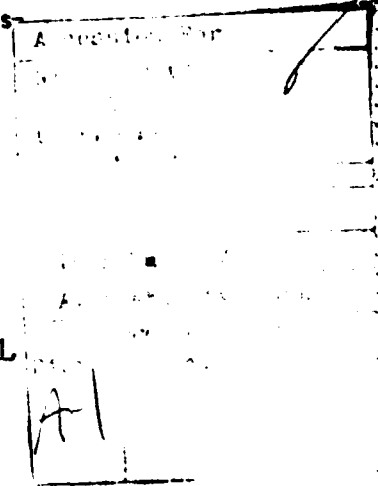
THERMAL SiO_2 – MOLYBDENUM INTERACTION

J. K. Srivastava and J. B. Wagner, Jr.
Center for Solid State Science
and Departments of Chemistry, Physics and
Mechanical and Aerospace Engineering
Arizona State University
Tempe, AZ 85287

Refractory metals and their silicides are of immense importance due to their application in VLSI semiconductor technology. Al and Au are the most common metals studied with regard to diffusion of metals in SiO_2 and their interactions with SiO_2. We have carried out some experiments to determine the Mo – SiO_2 interaction and the diffusion of Mo into SiO_2. McBrayer [1] has reported on the basis of his experiments that Pd, Au, Mo, Ta, W, Pt, Ti and Al are suitable candidates for VLSI gate and interconnect metallization. Recently, R. Pretorius, J. M. Harris and M. A. Nicolet [2] studied the reaction of thin metal films with SiO_2 substrates and concluded that Hf, Nb, Ti, V and Zr react with SiO_2.

In order to study the interaction between molybdenum and SiO_2, 1kA molybdenum was deposited by evaporation on films of SiO_2 1kA, 3kA and 20kA thick, thermally grown on silicon. Samples were cut into 1 cm^2 area rectangular pieces and were subjected to heat treatment under flowing argon or sealed evacuated tubes at 1000°C and 1100°C for different intervals of time. The technique used for analysis of reaction and diffusivity was the Rutherford Back Scattering technique. Spectra were analyzed by comparing the annealed samples with unannealed samples. Molybdenum appears to diffuse into SiO_2. From the spectra it appears that silicon is also diffusing out throug the SiO_2. From SEM and x-ray analysis, it is also obvious that at this high temperature molybdenum oxide is formed and at certain places, molybdenum accumulates. This work is still in progress and diffusion anneals will be carried out at lower temperatures to avoid the possibilities of "balling up" of the molybdenum.

REFERENCES

1. J. B. McBrayer, Diffusion of Metals in Silicon Dioxide (iii), 1983.

2. R. Pretorius, J. M. Harris and M. A. Nicolet, Solid State Electronics, 21, 667, 1978.

THIN SiO$_2$ FILMS: A STUDY BY HIGH RESOLUTION TRANSMISSION ELECTRON MICROSCOPY

By

J.K. Srivastava and J.B. Wagner, Jr.
Center for Solid State Science
and Departments of Chemistry, Physics and
Mechnical and Aerospace Engineering
Arizona State University
Tempe, Arizona 85287, USA

ABSTRACT

High resolution transmission electron microscopy studies of 7-8 nm thick SiO$_2$ thermally grown on silicon were carried out. Pore sizes of 5 to 8Å diameter were observed. These pores were randomly distributed throughout the silica film which were grown in both dry oxygen as well as in wet oxygen conditions. The pore sizes are consistent with those reported by Gibson and Dong [9]. Some fringes resembling crystalline SiO$_2$ were seen embedded in the predominantly amorphous structure. These fringes are very susceptible to the electron beam damage and disappear within a fraction of a second indicating that transformation of crystalline state to amorphous SiO$_2$ is very fast as has been found by Hobbs [11]. Crystalline SiO$_2$ in thermally grown silica has been reported by Evans and Chatterjee [12]. Crystallinity was not detected by X-ray analysis in our case. The presence of pores in the SiO$_2$ suggest possible diffusion of molecular oxygen through micropores. Observed crystallinity at the Si/SiO$_2$ interfaces provide evidence of ordering of SiO$_2$ at the   Si/SiO$_2$ interface. The crystallinity observed was in such a low concentration that it could not be an-

alyzed by x-ray techniques due to limitations of the x-ray dif-
fraction techniques.

INTRODUCTION

In a recent publication on a revised model for thermal oxida-
tion of silicon, Irene [1] stated that in early stages of silicon
oxidation at lower temperatures, transport occurs via micropores.
Rosencher, et al. [2] Pfeffer, et al. [3] and Castello, et al. [4]
using tracer techniques reported that molecular oxygen moves
through interstices in the SiO_2 during oxidation. Norton [5]
studied the diffusion of oxygen in fused quartz by a permeation
technique, using a mass spectrometer and suggested that oxygen
diffuses as molecular oxygen. There were differences in the values
of diffusivities obtained from different techniques used for mea-
surements of diffusion. Some workers who studied transport in SiO_2
have reported that transport in SiO_2 is via charged oxygen species
as well [6-8]. The oxidation kinetics of silicon have been studied
by various workers and the data have been fitted to a linear-para-
bolic model. The above linear parabolic model does not fit the
initial region of oxide growth up to about 500Å. This behavior
suggests that diffusion is not only Fickian diffusion but differ-
ent mechanisms of transport are occuring during oxidation as has
also been mentioned by Irene [1].

Gibson, et al. [9] first studied oxide films by high resolu-
tion bright field electron microscopy and observed the presence of
micropores in oxides grown in dry oxygen. Gibson suggested that
micropores may be the reasons for the differences in the proper-

ties of SiO_2 (for example dielectric breakdown voltage) thermally grown on silicon in dry and wet oxygen conditions. Irene [10], Costello and Tressler [4] proposed that these micropores can affect oxidation kinetics. In order to understand the mechanism in the initial stage of silicon oxidation and the causes for the differences in the electrical properties of two types of oxide films (dry and wet grown), high resolution TEM was carried out. The defocussing (defect of focus) technique was used to obtain phase - contrast in imaging. The details of defocusing are given in reference 9.

EXPERIMENTAL

Silicon wafers (100) p-type 14 - 22 ohm cm were obtained from Motorola, Inc. These wafers were cleaned by using hydrogen peroxide and a sulphuric acid mixture, to remove any organic impurity, and dried. These three inch wafers were oxidized in dry oxygen containing less than 1 ppm water and a few wafers were oxidized by passing oxygen over water maintained at 95°C, at a flow rate of 4.0 liters per minute. Silicon dioxide of different thicknesses ranging from 200 - 500Å were grown in both the cases at 1100°C. Oxide thicknesses were measured with an optical ellipsometer. 3mm diameter size discs were cut from the wafer using ultrasonic disc cutter Model 601 GATAN as prescribed for Transmission Electron Microscopy. These samples for microscopy were prepared by jet etching first by chemical etching and then by ion milling. The oxide was protected by using wax. Chemical etching was done using initially 1:10 $HF:HNO_3$ mixture and finally with a dilute solution

of $HF:HNO_3$ to prepare a uniform layer. Final thinning of the disc was done using ion milling until the formation of a tiny hole at which point several areas of 7 - 9 nm thick SiO_2 were produced.

TEM images were taken with a TEM-200CX electron microscope. The maximum resolution of the microscope is 2.5Å at the maximum excitation of the objective lens and maximum magnification. The images were taken under axial illumination with a beam divergence of 15mrad. The pictures were taken at different defocus to see the contrast in the images. The electron source was a precentered LaB single crystal filament. The details regarding instrument, image formation, and characteristics are given in the Instruction Manual of TEM-200CX.

RESULTS AND DISCUSSION

Figure 1 shows the images of the dry SiO_2 film which were taken at different values of defocus and shows a contrast reversal in images. The pictures show the amorphous structure of SiO_2. Arrows points show the micropores, which are distributed randomly in the SiO_2 film as shown in Figure 2. The average pore size was estimated to be between 5 - 8Å. These pore sizes are in good agreement with the theoretically calculated pore size for 8 nm thick oxides which are prevailing in this experiment using relation d min > 1.8 (Ω T) 1/4 (8), where d is diameter of pores, Ω is atomic volume and T is the film thickness. The diameters of the pores in the pictures varies with different values of defocus Z, which confirms the existence of micropores in the film. The mean distance between two pores is normally 6 nm and the density

of pores is approximately 4.2×10^{12} cm^{-2} which is in good agree-
ment with the calculated values by Irene [1] for 8 nm thick SiO_2
film. The SiO_2 grown under the wet conditions shows the same type
of behavior. The formation of pores in SiO_2 may be due to several
possible mechanisms. The stress and strain in the silicon during
oxidation may lead to the formation of cracks or pores. Secondly,
the origin of micropores may also be due to the spacing between
the tetrahedrals and interstices, thirdly during oxidation of sil-
icon the series of vacancies of the atoms or planar defects may
also give rise to micropores.

SiO_2 grown in dry oxygen exhibit some fringes as shown in
Figure 3. These fringes which resemble crystalline SiO_2 were found
embedded in the predominantly amorphous structure. These fringes
are very susceptible to the electron beam and disappear within a
fraction of a second, indicating that the transformaiton of the
crystalline form to amorphous SiO_2 is very fast as has been obser-
ved previously by L.W. Hobbs [11]. There is also some evidence of
ordering of crystalline SiO_2 in the amorphous structure. The max-
imum width of the crystaline region is about 30 - 40Å wide and d-
spacing between each fringe is 4.16Å. Both these observations sug-
gest that crystalline SiO_2 is present in amorphous SiO_2 grown in
dry oxygen, but it is in such a low concentration that it was not
detected by x-ray techniques. The presence of crystalline SiO_2
(crystobalite) in thermally grown SiO_2 in dry oxygen has been pre-
viously reported by Evans and Chatterjee [12]. Such fringes were
not observed in the wet oxide. The presence of fringes may be due
to ordering at crystalline SiO_2 at the Si/SiO_2 interface. In order to

study the transformation from amorphous to crystalline silica (if any) images were taken at different time intervals, but due to the high electron beam density loss, transformation could not be observed.

The 5 - 8Å micropores present in both the types of SiO_2 at the thickness of 500Å SiO_2 layer are large enough to allow the permeation of oxygen molecules or ions. The diameter of oxygen molecule and ion is 3.6Å and 1.3Å respectively. These results are in agreement with the data of Gibson for silicon formed in dry oxygen [9] and calculated values by Irene [10]. Because both the wet and dry formed SiO_2 exhibit the same size pores and same density of pores, it is difficult to attribute the large difference in oxidation kinetics and conductivities of the resulting oxides to transport down micropores. Rather these results suggest that the parallel process of bulk diffusion is affected by water vapor. Further work is needed on wet-grown SiO_2 films.

REFERENCES

1.   E. A. Irene, J. Appl. Phys., 54, (9), September, 1983.

2.   E. Rosencher, A. Straboni, S. Rigo and G. Amsel, Apply Phys. Lett., 34, 254 (1979).

3.   R. Pfeffer and M. Ohring, J. Appl. Phys., 52, 777 (1981).

4.   J. S. Costello and R. E. Tressler, J. Electrochem. Soc., 131, 1944 (1984).

5.   F. L. Norton, Nature, 101, 701 (1961).

6.   P. J. Jorgensen, J. Chem. Phys., 37, S74 (1962).

7.   F. M. Folkes, et al., Abs. No. 166, Electrochem. Soc. Meeting, St. Louis, Missouri, May 6 - 11, 1980.

8.   J. K. Srivastava, M. Prasad and J. B. Wagner, Jr., Abs. No. 305, Electrochem. Soc. Meeting, Washington, DC, October 9 - 14, 1983.

9.   J. M. Gibson and D. Dong, J. Electrochem. Soc., 125, 2722 (1980).

10.   E. A. Irene, J. Electrochem. Soc., 125, 1708 (1978).

11.   L. W. Hobbs, Proc. of the 41st Annual Meeting of Electron Microscopy Society of America, pp. 346, 1983.

12.   J. W. Evans and S. K. Chatterjee, J. Phys. Chem., 62, 1062 (1958).

FIGURE CAPTIONS

Fig. 1 (a,b)   High magnification images of dry oxide films at different values of defocus (z).

Fig. 2 (a,b)   High magnification images of dry oxide films at different values of defocus (z). Showing contrast in images. Somes micropores are shown by arrows.

Fig. 3   High magnification image of a dry oxide film showing some crystalline fringes embedded in amorphous SiO_2.
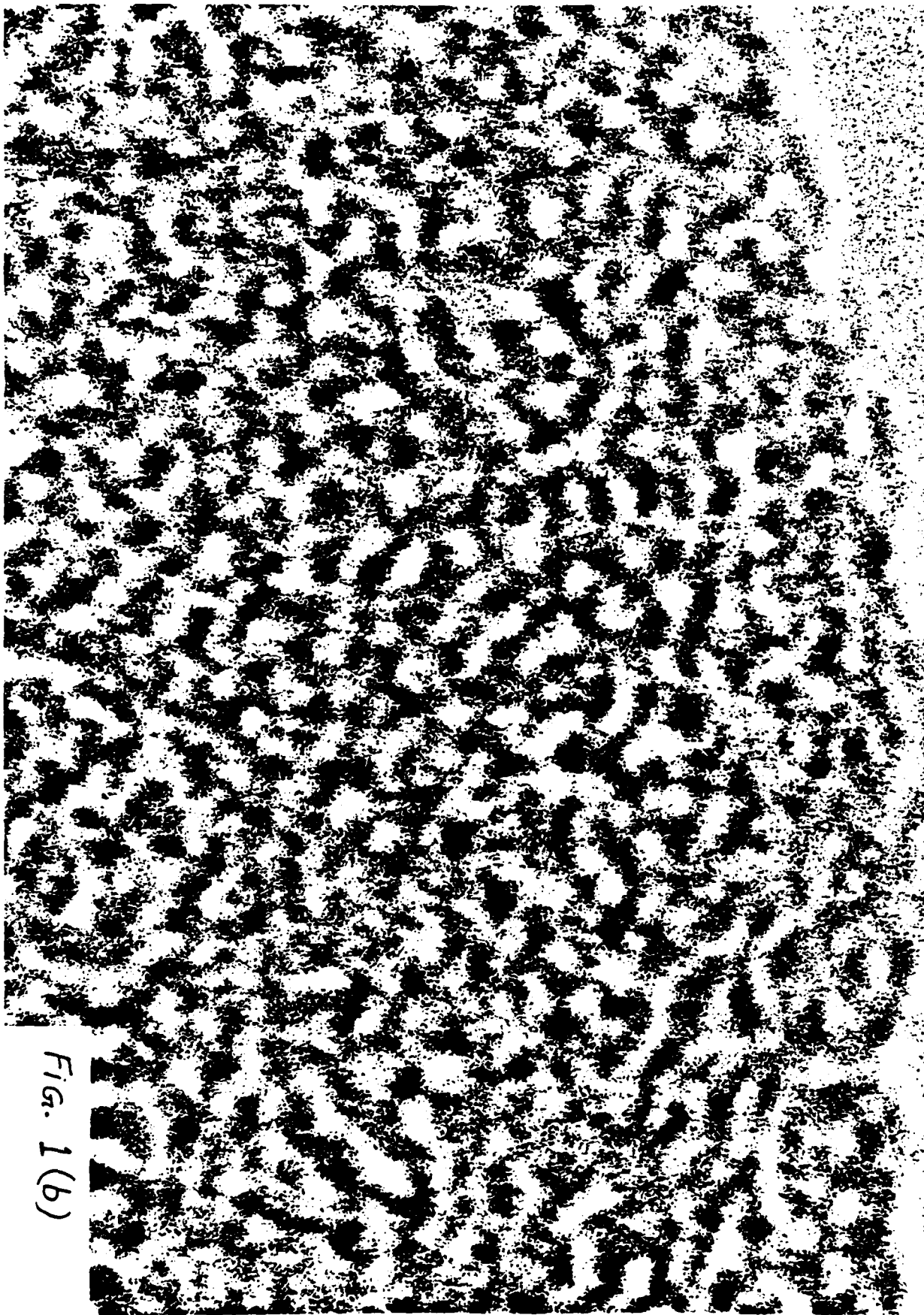
+Z
17000000 X

F I G. 1 (a)
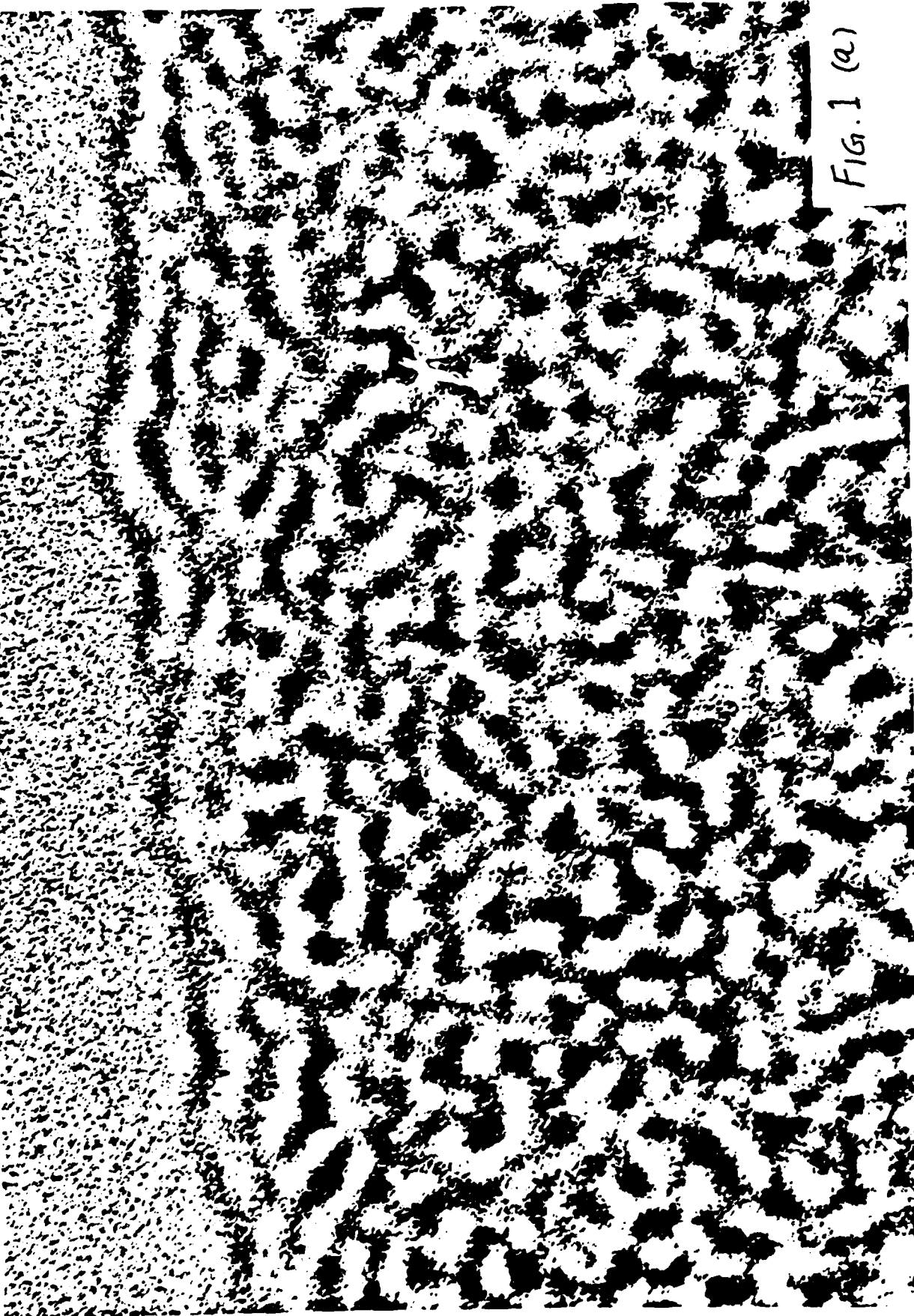
DRY OXIDE
- Z
1700000 X

Fig. 1 (b)

DRY OXIDE
LZ
7 000 000 X
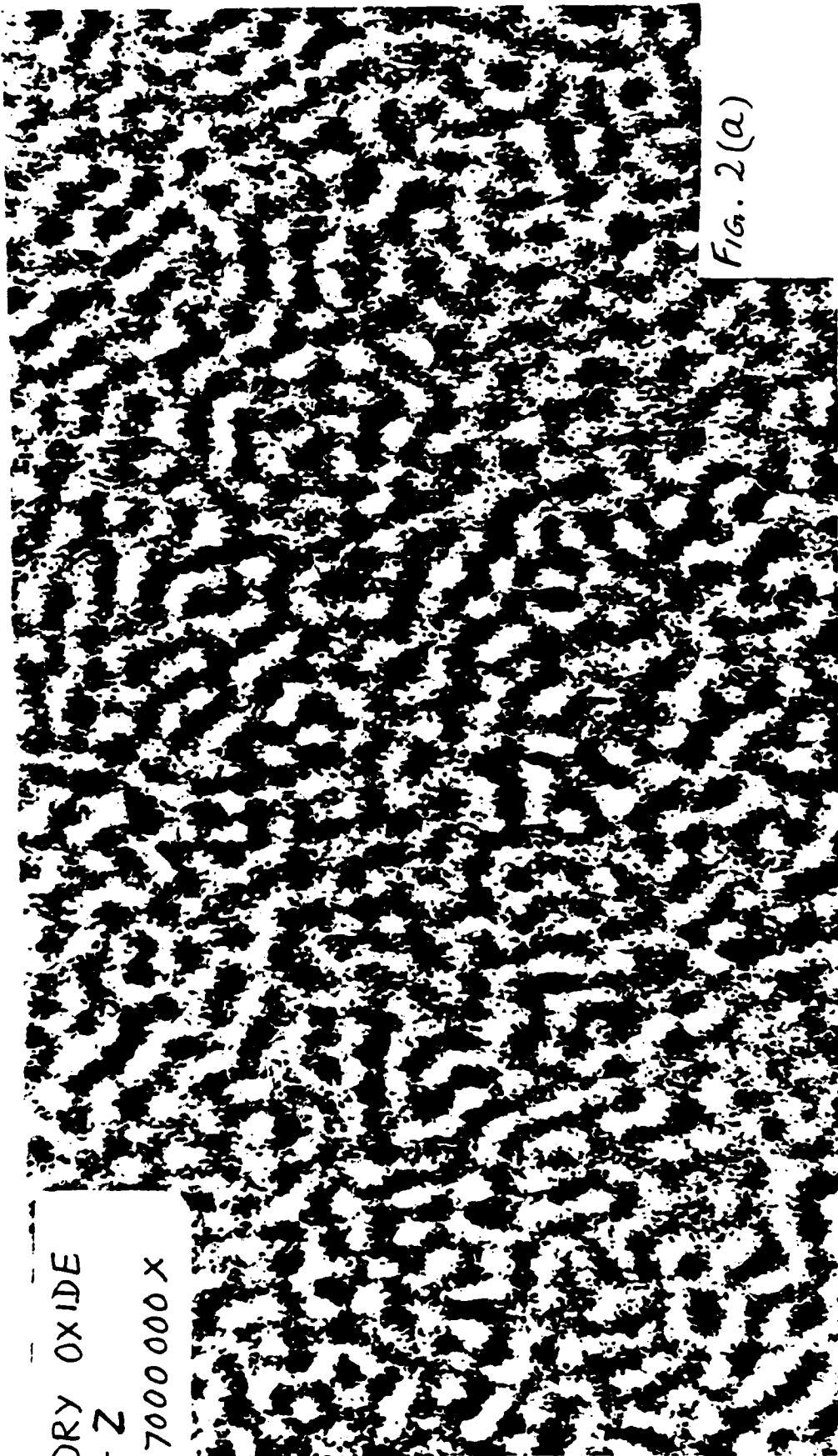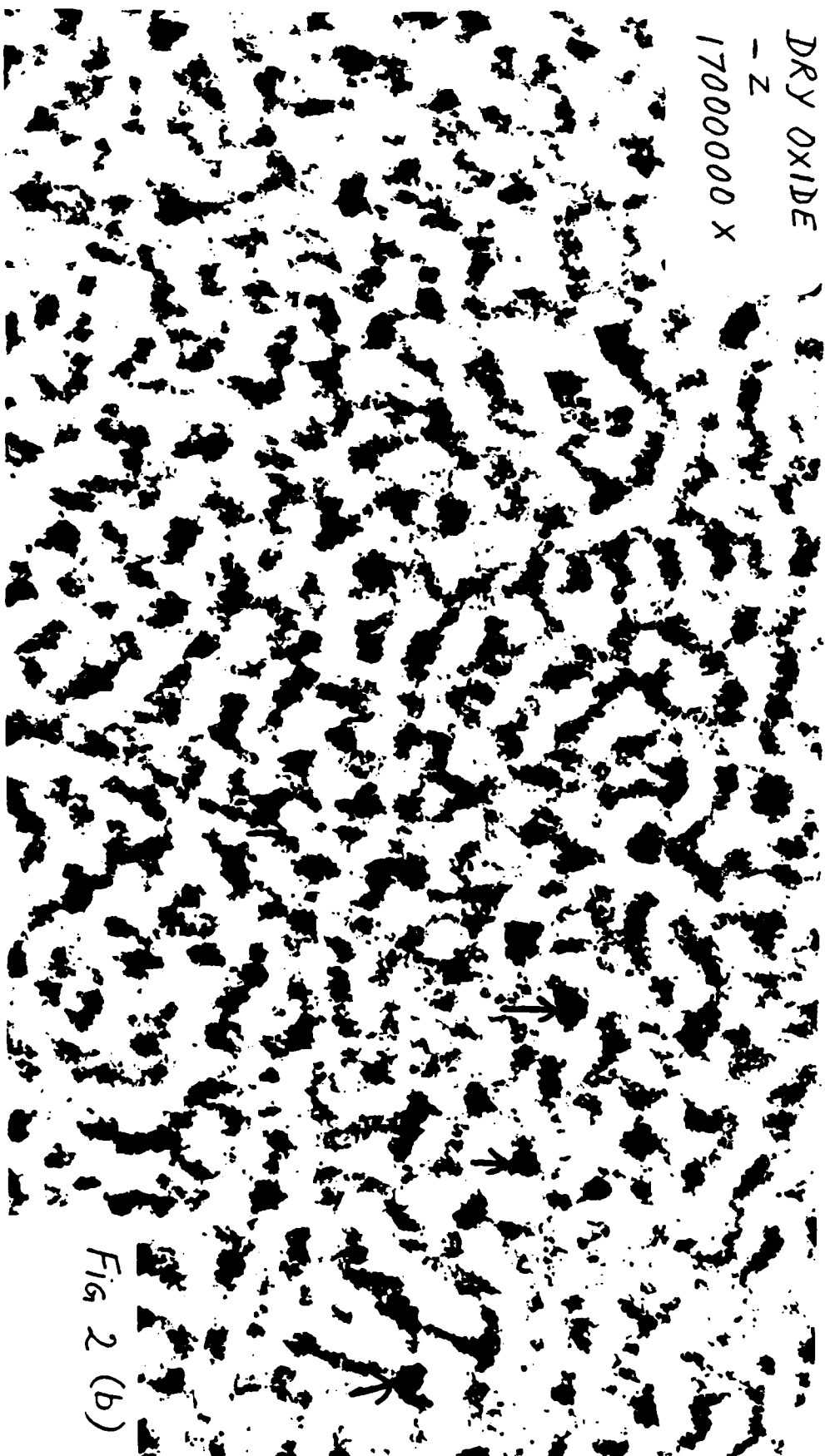
FIG. 2(a)

DRY OXIDE
-Z
17000000 X

Fig 2 (b)

FIGURE. 3

4·16 A°

30A°

DRY OXIDE
170 00000 X

TRANSPORT NUMBER MEASUREMENTS IN SILICA*

J.K. Srivastava, V.B. Tare and J.B. Wagner, Jr.**
Center for Solid State Science and
Departments of Chemistry, Physics and
Mechanical and Aerospace Engineering
Arizona State University
Tempe, AZ   85287 U.S.A.

ABSTRACT

Using an open circuit emf method the average transport number for ions, t_i, has been determined for quartz crystals, for vitreous silica and for amorphous silica grown thermally on silicon. Results for all types of silica show that $\bar{t}_i$ increases with temperatures between about 550° and 950°C.

INTRODUCTION

Silica exists in three commonly occurring forms viz, crystalline, amorphous and supercooled liquid or vitreous state [1]. Schmalzried [2] reported that at 1000°C and between 10^{-16} and one atmosphere of oxygen pressure the transport number of ions in silica glass is close to unity.   For silica thermally grown on silicon, Jorgensen [3] and Mills and Kroger [4] suggested that the charges associated with the transport of oxygen ions through SiO_2 are less than the conventionally accepted values of four per mole of oxygen under certain conditions.

Diffusion of oxygen through silica has been studied by several investigators [5]. The results indicate that the diffusion of oxygen in quartz is strongly anisotropic.   The diffusion of oxygen

---

through various forms of silica has been suggested to be due to transport of oxygen as an uncharged molecule or as $\bar{0}_2$ or as $\bar{\bar{0}}_2$ [4]. When bulk diffusion of ions and electrons (to preserve electroneutrality) governs the kinetics of oxidation of silicon, the rate of oxidation can be calculated by C. Wagner's equation [6], provided the transport number of ions and electrons through the growing oxide layer are precisely known. The main reason for the observed discrepancy between the experimentally determined rates of oxidation and the rates estimated from the available data on transport number and the diffusion of oxygen is possibly the lack of reliable information of the transport numbers and diffusivities.

The present paper describes the measurement of transport number by an emf method [2] in all three different types of silica, viz single crystal quartz, vitreous silica and amorphous silica thermally grown on single crystal Si. This method essentially involves measurements of open circuit emf of a cell in which silica is an electrolyte separating two different oxygen partial pressures. In case of silica thermally grown on silicon the partial pressure of oxygen at Si/SiO_2 interface is the dissociation pressure of SiO_2. The other oxygen pressure was fixed by a metal/metal oxide mixture. For the vitreous and single crystalline quartz the oxygen pressures on two sides of the electrolytes were fixed by a metal/metal oxide mixtures.

EXPERIMENTAL PROCEDURE

Single crystalline quartz used in the present investigation was obtained from Bell Laboratories and had <010> growth directions. It

was free from sodium and potassium impurities (less than detectable level <1 ppm). The principle impurities were, Fe 30 ppm and Al 30-50 ppm. Rectangular pieces of 1.5 x 1.5 x .2 cm with <010> orientation were cut from a large crystal with the help of a diamond saw. The pieces were cleaned with a HF-water mixture, degreased with acetone and finally washed with distilled water and again cleaned in an ultrasonic cleaner in acetone.

Vitreous and SiO_2 thermally grown on silicon were obtained from Motorola. 20 kÅ thick SiO_2 was thermally grown on n-type silicon <100> with 3-4 ohm cm resistivity. The vitreous silica was 1 mm thick. These were cut into pieces of similar dimensions as the crystalline quartz, and were also cleaned by the same procedure described for crystalline quartz. The sample was of semiconductor grade purity.

Three different metal/metal oxide mixtures used to obtain different partial pressures of oxygen were Cu/Cu_2O, Ni/NiO, Fe/FeO. These were prepared by using the metal and its oxide powder both of 99.999% obtained from Alfa Products. They were mixed in 1:1 volume ratio in an agate mortar and pressed into pellets of 3 mm thickness and 1 cm diameter in a steel die. These pellets were sintered for 15 hours in purified argon at temperatures varying from 500° to 700° C to increase their density and improve the mechaical strength. These were then lightly polished with 3/0 emery paper and cleaned with acetone before use.

To obtain the open circuit emf, the silica pellets were sandwiched between two different metal/metal oxide pellets. The whole

assembly was held together by means of a spring assembly and an alumina sample holder. The details were similar to those described elsewhere [7]. Platinum wires, spot welded to platinum foils pressed on the metal/metal oxide electrodes, were used as leads to measure open circuit emf. A Pt - Pt + 10% Rh thermocouple placed very near to the electrolyte was used to measure temperature. The whole assembly was introduced in another alumina tube in which a continuous flow of argon purified by passing it over Drierite, phosphorous pentoxide and copper heated at 400°C. The complete assembly was kept in a resistance furnace whose temperature was controlled within $\pm 1°C$ with a proportional temperature controller. The cell was electrically shielded from the furnace to avoid external stray pick up.

The open circuit emf was measured using 117 Keithley Digital Voltmeter with an impedence of 10 MegOhms. The following cell configurations were used to obtain the open circuit voltages.

Cu/Cu_2O	Quartz crystal	Ni/NiO	I
Fe/FeO	Quartz crystal	Ni/NiO	II
Fe/FeO	Vitreous silica	Ni/NiO	III
Pt,Si	Thermally grown SiO_2	Ni/NiO	IV

Measurements were repeated on at least two cells of the same cell configuration. Measurements were restricted to 900°C because above this temperature there was some evidence of the electrode-electrolyte reaction particularly in Cell I at the quartz $Cu-Cu_2O$ interface. The emf values were however reproducible during several heating and cooling cycles if the measurements were restricted to temperatures below 900°C.

RESULTS AND DISCUSSION

According to C. Wagner [6], the open circuit emf, E, of the above cells is given by

$$E = \frac{1}{nF} \int_{\mu'_{O_2}}^{\mu''_{O_2}} t_i \cdot d\mu_{O_2} \tag{1}$$

where n is the charge per mole of oxygen ion migrating through the sample, F is Faraday's constant and μ'_{O_2} and μ''_{O_2} are the chemical potentials of oxygen on each of the two sides of the electrolyte. The derivation of Eq. (1) assumes transport by ions.

The chemical potentials are given by,

$$\mu_{O_2} = \mu^{\circ}_{O_2} + RT \ell n P_{O_2} \tag{2}$$

where $\mu^{\circ}_{O_2}$ is the chemical potential of oxygen in its standard state 1 atm of oxygen. Thus Eq. (1) can be written as

$$E = \frac{RT}{nF} \int_{P'_{O_2}}^{P''_{O_2}} t_i \cdot \frac{dP_{O_2}}{P_{O_2}} \tag{3}$$

If an electrolyte is completely ionic i.e. $t_i = 1$, Eq. (3) becomes

$$E_{ion} = \frac{RT}{nF} \ell n \frac{P''_{O_2}}{P'_{O_2}} \tag{4}$$

Where E_{ion} is the theoretical voltage as calculated. The P'_{O_2} and P''_{O_2} can be easily calculated from the free energies of formation of respective oxides used to fix the oxygen pressures.

However, if $t_i \neq 1$ the voltage will, in general, be a complex function of oxygen pressure (see reference 2). As a first approximation however, we may take it outside the integral by replacing t_i with $\bar{t}_i$, the average transport number at oxygen pressures between P'_{O_2} and P''_{O_2}.

Dividing equation (3) by equation (4) the expression for average transport number is,

$$\bar{t}_i \quad = \quad \frac{E_{obs}}{E_{ion}} \qquad (5)$$

where E_{obs} is the measured open circuit emf.

The data obtained on all the cells are tabulated in Table I. To estimate E_{ion}, free energies of formation of the respective oxides were taken from the data compiled by Turkdogan [8]. Also in calculating E_{ion}, the value of n is assumed to be 4 per mole of oxygen.

Figure 1 shows the observed as well as theoretical open circuit emfs (E_{ion}) for Cell I. The corresponding values of $\bar{t}_i$ are shown in Table I. It can be seen that the $\bar{t}_i$ for quartz is nearly equal to 1 only between 700° - 900°C. The values of $\bar{t}_i$ at temperatures less than 700°C, deviate considerably from unity.

Figure 2 shows the open circuit emf, E_{obs}, for Cells II and III as a function of temperature. E_{ion} is also shown for comparison. In this oxygen pressure range also crystalline quartz has $\bar{t}_i \cong 1$ at the temperatures above 700°C. The values of $\bar{t}_i$ drop steeply below 700°C. Data above 900°C could not be obtained because of the possible reaction of electrolyte with the electrodes. $\bar{t}_i$ for vitreous silica (Cell III) is much lower than 1 for all tempera-

tures (see Table I). The transport number however, increases with increase in temperature and attains a maximum value of 0.7 in the temperature range of $800°$ - $900°C$.

A similar trend in the variation of average transport number with the increase in temperature is observed for Cell IV (Fig. 3). In this case, the average oxygen pressure is however very low. The maximum in average transport number is 0.4 and occurs also in the temperature range $750°$ - $950°C$, although the scatter in the data is very large.

As mentioned earlier, the average transport number has been obtained assuming the values of n in equation 4 to be 4. In the temperature range $700°$ - $900°C$, these average ionic transport numbers were found to be maximum values for all the three forms of silica samples. The transport number of crystalline quartz is close to unity, while for vitreous silica $\bar{t}_i$ = 0.7 and for SiO_2 thermally grown on Si it is ~0.2-0.39. A value of $\bar{t}_i$ = 1 for cry-stalline quartz in the temperature range of $700°$ - $900°C$ suggests that, the assumption for the value of n = 4 is justified. Lower values of $\bar{t}_i$ for the vitreous silica at the same average oxygen activity as that for crystalline quartz may be because of the electronic conductivity or because of the deviation of n from 4. Vitreous silica is considered to be a supercooled liquid. Liquid-like structures generally favor higher ionic transference numbers. It is, therefore, suggested that lower transference number in vit-reous SiO_2 may be due to a value of n different than 4. In other words, the oxygen ions migrating in these samples may have charges varying from almost 0 to 4 per molecule as has been suggested earlier [5].

The small ionic transference number for SiO_2 thermally grown in silicon can also be explained in a similar way. In fact, this ionic transport number is so low that the possibility of the transport of neutral oxygen cannot be ruled out [9].

The above explanation is consistant with the one offered by several investigators on transport properties of SiO_2. However, further experiments are essential to resolve the nature of transporting species unambiquously. The ionic transport number in SiO_2 thermally grown on Si, obtained independently by polarization technique [7], is found to be approximately 0.9 in the temperature range of 750° to 875°C. This is consistent with the hypothesis that uncharged oxygen is involved in the transport as has been reported by Costello and Tressler [10] from oxidation studies at 1000°C. The polarization technique involving measurements of current-voltage characteristics on a material where the electronic conductivity is due to the electrons only, is influenced bv the transport of only charged species whereas, as mentioned earlier, the open circuit voltage data depends upon the effective charges 'n' in the migrating oxygen.

REFERENCES

[1] F.A. Cotton and G. Wilkinson, Advanced Inorganic Chemistry, John Wiley and Sons (1980).

[2] H. Schmalzried, Z. Physik Chem. Naue Folge, $\underline{38}$, (1963) 87.

[3] P.J. Jorgensen, J. Chem. Phys., $\underline{37}$, 874 (1962).

[4] T.G. Mills and F.A. Kroger, J. Electrochem. Soc., $\underline{120}$, 1582, (1973).

[5] G.H. Frischat, Ionic Diffusion in Oxide Glasses, Trans. Tech. Publication, 29, (1976).

[6] C. Wagner, Phys. Chem. (B), $\underline{21}$, 25, 1933.

[7] J.K. Srivastava, M. Prasad and J.B. Wagner, Jr., Extended Abstract No. 305, Electrochem. Soc. Meeting Washington, October 9-14, 1983.

[8] E.T. Turkdogan, Physical Chemistry of High Temperature Technology, Academic Press, 1980.

[9] A.G. Revesz, J. Non Crystalline Solids, $\underline{4}$, 347, (1970).

[10] J. A. Costello and R. E. Tressler, J. Electrochem. Soc., $\underline{131}$, 1944 (1984).

TABLE I

Ionic transport number for all these forms of silica estimated from the experimentally observed (E_{obs}), and the theoretically calculated (E_{ion}) emfs of Cells I to IV at various temperatures.

CELL	T°C	E_{obs} (mV)	E_{ion} (mV)	$\bar{t}_i$
I	545	75	284.88	0.26
Cu/Cu$_2$O	590	110	281.42	0.39
Quartz	600	125	280.59	0.44
crystal	675	150	274.90	0.58
Ni/NiO		160		
	725	235	271.07	0.90
		245		
	800	265	265.32	0.98
	850	235	261.48	0.95
		250		
	900	245	257.65	0.97
		250		
II	530	40	236.03	0.16
Fe/FeO	570	75	240.50	0.31
Quartz	640	155	248.41	0.62
Ni/NiO	675	190	252.30	0.75
	700	220	255.16	0.86
	725	250	257.97	0.99
	790	265	265.28	0.99
	840	265	271.13	0.97
III	645	130	248.97	0.52
Fe/FeO	728	162	250.31	0.62
Vit. Silica	790	185	265.28	0.69
Ni/NiO	865	200	274.85	0.72
	915	201	279.35	0.71
	950	208	283.28	0.71
IV	625	125	1121.08	0.11
Pt, Si		127		
Thermally	700	235	1120.39	0.20
Grown SiO$_2$	740	320	1120.01	0.28
Ni/NiO	750	375	1119.92	0.33
	850	445	1118.99	0.39
	950	438	1118.06	0.39

FIGURE CAPTIONS:

Figure 1   Observed (E_{obs}) and Theoretical (E_{ion}) open circuit
             emf's (OCE) of Cell I, Cu, Cu_2O|Quartz Crystal|Ni, NiO,
             in the temperature range 550° to 900° C.

Figure 2   Observed (E_{obs}) and Theoretical (E_{ion}) open circuit
             emf's (OCE) of Cell II, Fe, FeO|Quartz Crystal|Ni, NiI
             and Cell III, Fe, FeO|Vitreous Silica|Ni, NiO in the
             temperature range 500° - 950°C.

Figure 3   Observed (E_{obs}) open circuit emf's (OCE) of Cell IV,
             Pt, Si|Thermally Grown SiO_2|Ni, NiO in the temperature
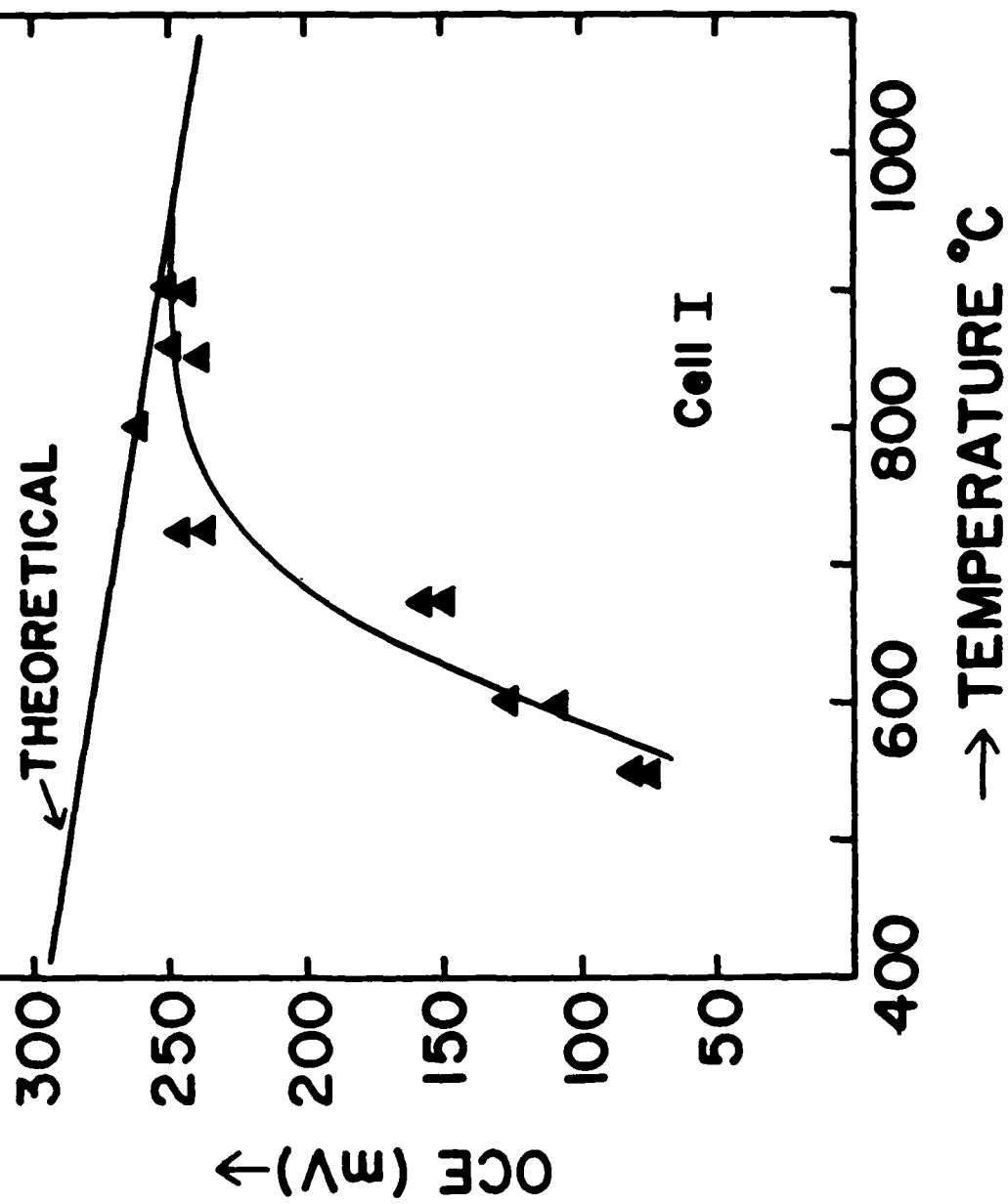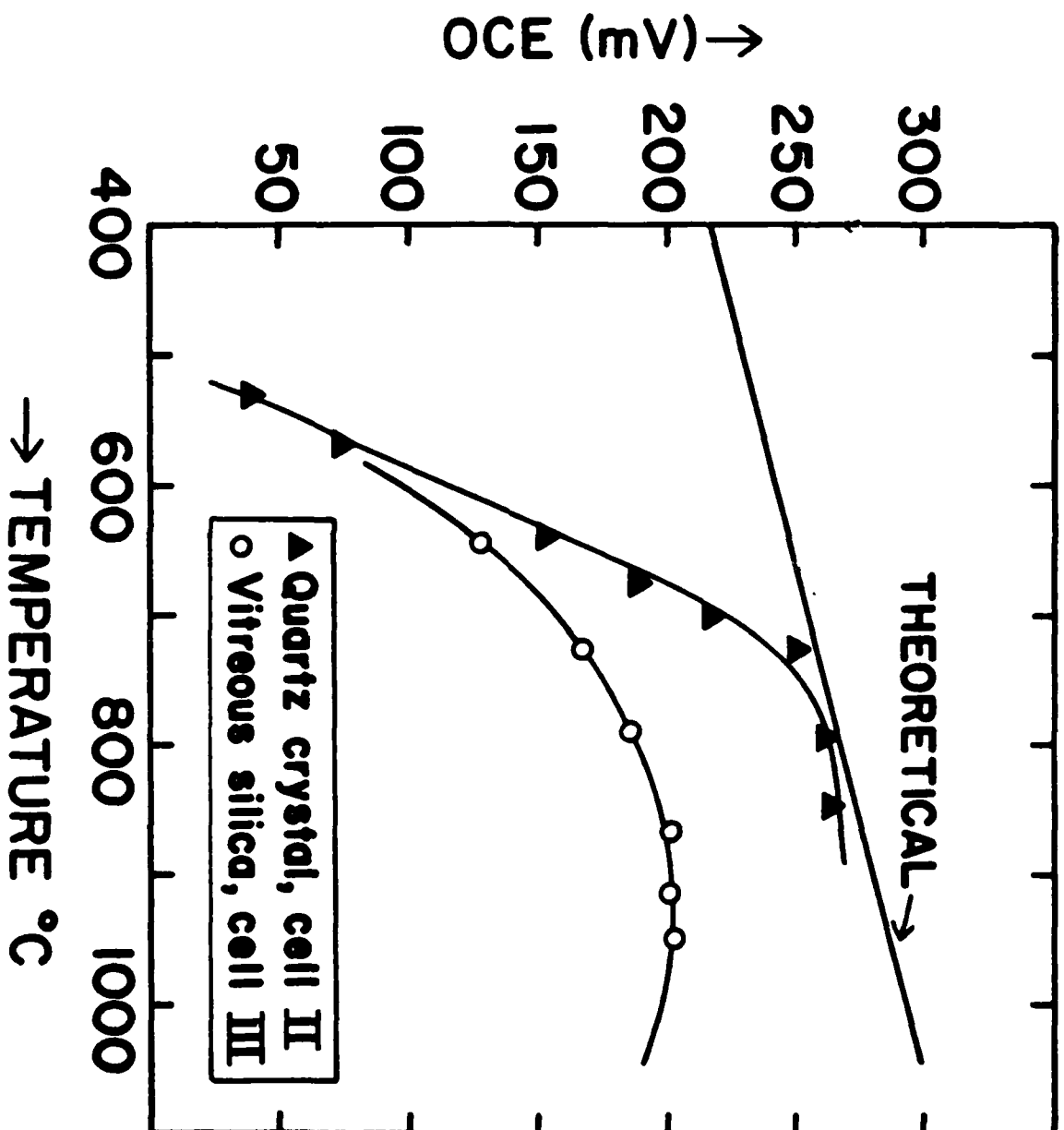   range 600° to 950°C.

Figure 1   Srivastava, Tare & Wagner

Figure 2   Srivastava, Tare and Wagner
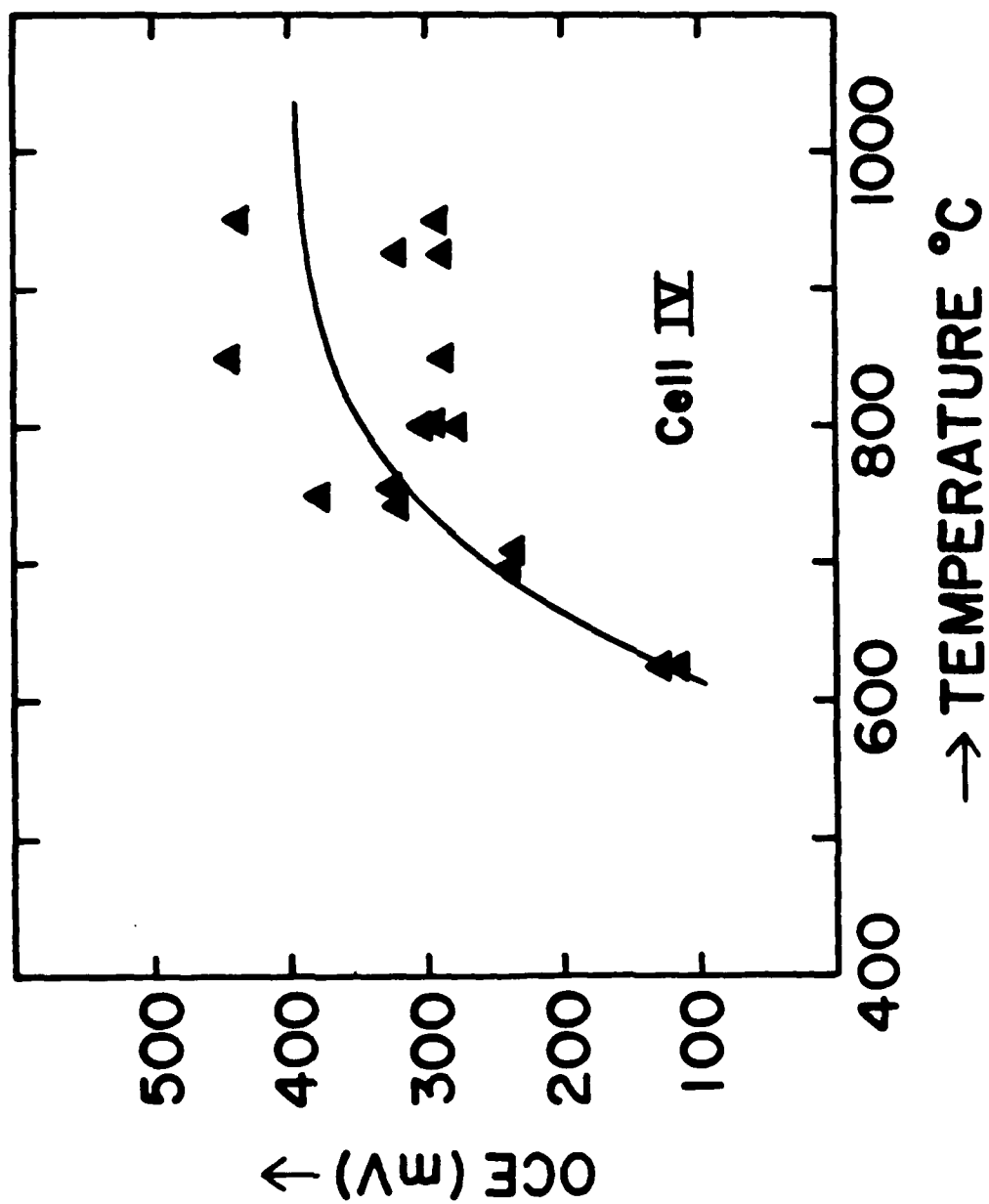
OCE (mV) →

THEORETICAL →

▲ Quartz crystal, cell II
○ Vitreous silica, cell III

→ TEMPERATURE °C

Figure 3   Srivastava, Tare and Wagner

The figure shows a graph plotting OCE (mV) on the vertical axis against TEMPERATURE °C on the horizontal axis.

Vertical axis (OCE (mV)): 100, 200, 300, 400, 500

Horizontal axis (→TEMPERATURE °C): 400, 600, 800, 1000

Cell IV

ELECTRICAL CONDUCTIVITY OF SILICON DIOXIDE THERMALLY GROWN ON SILICON

J.K. Srivastava, M. Prasad and J.B. Wagner, Jr.
Center for Solid State Science
Depts. of Physics, Chemistry and Mechanical/Aerospace Engineering
Arizona State University, Tempe, AZ U.S.A.

ABSTRACT

D.C. and A.C. electrical conductivities of silicon dioxide thermally grown on p-type (boron doped) and n-type (phosphorous doped) silicon have been measured in the temperature range of 25°C to 1100°C. Total D.C. conductivities varied from 10^{-9} to 10^{-16} ohm^{-1} cm^{-1} in the temperature range of 25°C to 960°C. Arrhenius plots for total D.C. conductivities of SiO_2 grown on both the substrates, exhibit two regions. Below 450°C the conductivities were independent of temperature and are suggested to be governed by impurities. Above 450°C, the total D.C. conductivities increased with increase in temperature. The activation energies of conduction in the temperature range 500°C to 960°C were estimated to be 1.65 eV and 2.10 eV for SiO_2 grown on p-type and n-type silicon respectively. D.C. polarization measurements carried out in this temperature range suggest that conduction in SiO_2 is ionic as well as electronic. The ionic conduction is believed predominantly to be due to the transport of oxygen ions.

A.C. conductivities were also measured in the temperature range of 550°C to 1100°C. The activation energies for the conduction in this temperature range were estimated to be 1.55 eV for SiO_2 on p-type

silicon and 1.86 eV for SiO_2 on n-type silicon. These values are in close agreement with the values reported in the literature. A.C. conductivity of SiO_2 grown on n-type silicon was found to be lower than that of SiO_2 grown on p-type silicon.

INTRODUCTION

In semiconductor and integrated circuit devices, silicon dioxide is grown thermally on silicon where it is used not only as an insulator, but also as a masking layer. The transport properties of SiO_2 thermally grown on silicon have therefore been studied by several investigators. Most of these studies have been restricted to a specific temperature region, depending on specific applications. Norton [1] and Sucov [2] independently studied the diffusion of oxygen in bulk fused silica. More recently, Irene [3] studied transport phenomena in thin SiO_2 films during oxidation of silicon. There is, however, considerable disagreement between the values of diffusivity determined directly and those estimated from the oxidation kinetics.

From marker studies [4-6], it is generally agreed that the inward migration of oxygen through the SiO_2 to the Si/SiO_2 interface determines the kinetics of transport through SiO_2. The mobile oxidant species in SiO_2 films has still not been uniquely determined. According to Revesz [7, 8], the oxygen migrating through SiO_2 during oxidation may not necessarily be a charged species. Neutral oxygen molecules may migrate through microheterogenities, or the 'channels' formed from d π and p π bonds [9] of silicon and lone pair electrons of the oxygen atom respectively. Jorgensen's experiment [6] on the oxidation of silicon with and without applying an electric field,

suggests that the oxygen diffusing through SiO_2 is negatively charged and that between 727 - 879°C SiO_2 is a mixed conductor with 0.4 as the value of ionic transference number (t_i). However Raleigh [10] reported that Jorgensen's data could be equally well explained by electrolysis at each Si/SiO_2 interface.

Mills and Kroger [11] measured electrical conductivity up to a temperature of 700°C to determine the mobile species in SiO_2 and concluded that the mobile species was charged oxygen. The extrapolated value of the total conductivity reported by Mills and Kroger [11] was several orders of magnitude higher than that reported by Raleigh [10] at 850°C and two orders of magnitude higher than the A.C. conductivity values of vitreous silica reported by Tripp, et al. [12].

In spite of the large number of investigations, the exact nature of the transporting species through SiO_2 during oxidation is still unsettled. Similarly, there is considerable discrepancy between the data reported on the rate of oxidation of silicon, the diffusivities through the product layer and the conductivity. Because of the inconsistencies in the reported data and the lack of conductivity data at higher temperatures, the present investigation was undertaken. Transport number measurements were made by electrical conductivity and open circuit emf methods on SiO_2 thermally grown on silicon substrates.

EXPERIMENTAL

1 kÅ to 5 kÅ thick SiO_2 films were grown thermally at one temperature, 1050°C, in dry oxygen on boron doped p-type silicon <100> (14-22 ohm cm) and phosphorous doped n-type silicon <100> (3.3 ohm cm) by Motorola, Inc. One side of

these wafers was etched to provide a clean silicon surface. Platinum or molybdenum was sputtered thereon to provide an electrical contact. These oxidized wafers were cut into 1 x 1 cm square pieces and pressed together with oxide surface to oxide surface, to yield a symmetrical cell (A) in an oxygen activity corresponding to the Si/SiO_2 equilibrium. For comparison, a 3 k$\overset{\circ}{A}$ oxide thickness on p-type silicon was obtained, in this laboratory, by passing O_2 over hot water maintained at 95 °C then over Si at 1100°C at a rate of 4 liters per minute. A.C. conductivity of this SiO_2 was also measured using a cell, configuration (A). For polarization and open circuit emf measurements, 1 k$\overset{\circ}{A}$ thick platinum or molybdenum, was sputtered on the SiO_2 side and assembled as an asymmetrical cell (B).

The cell configurations (A) and (B) were:

Symmetrical cell (A) - for total A.C. and D.C. conductivity;

M | Si | SiO_2 | Si| M
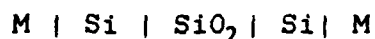
where M is Pt or W

Asymmetrical cell (B) for polarization and emf measurements

M | Si | SiO_2 | M
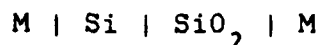
where M is Pt or W.

The apparatus consisted of a double walled silica tube and a sample holder made of quartz with inlets and outlets for gases in each jacket, electrical circuits and a Lindberg heavy duty furnace. Platinum or tungsten (~0.12 mm thick) in the form of disc or rectangular plate was used as electrode material. The tubular quartz

furnace was electrically shielded by grounding a closely wound Kanthal wire around the tube. Shielded cables were used for external leads. Alumina discs were used in order to avoid any possible contact between the sample and the sample holder.

Each cell was positioned between platinum electrodes and pure dry argon, (oxygen less than 1 ppm) was allowed to circulate in each jacket of the silica tube. The argon in the outer jacket was used to eliminate the possible diffusion of H_2O through the quartz wall and into the sample. The samples were annealed at $600°C$ for about 12 hours prior to measurements. After such annealing, it was found that adjoining SiO_2 surfaces in Cell (A) were bonded together.

D.C. conductivity was measured with Cell (A) using 1000 - 3000 Å thick SiO_2 by connecting the samples in series with a 10^6 to 10^{11} ohm precision glass encapsulated standard carbon film 'HiMEG - Resifrom. 0.1 to 1.3 volts were applied using a Keithly 260 nanovolt source. The voltage drop across the standard resistor was measured with a Keithly 604 differential electrometer.

Electronic conductivity was measured using the polarization technique described by Wagner [13, 14] using cell configuration (B), as suggested by Raleigh [10]. In this experiment, the positive potentials of 0.1 to 0.8 volts were applied on the SiO_2/Pt side using a Keithly 260 nanovolt source and measuring the voltage drop across the standard resistor with an electrometer.

A.C. conductivity was measured using cell configuration (A) for different thicknesses of SiO_2 on silicon in the temperature range of 550°C to 1100°C, using a Wayne Kerr Model-211 conductivity bridge.

The conductivities were also measured at different frequencies (50 Hz - 1 kHz) at various temperatures.

RESULTS and DISCUSSION

Symmetrical cell (A)

The values of current (I) at different applied voltages (V) were obtained, initially in the temperature range 500 - 960°C. The measurements were subsequently extended to temperatures between 500°C and 25°C. At higher temperatures and higher applied voltages, the current was found to change with time for the same applied voltage. A typical current time curve at 860°C for SiO_2 grown on n-type silicon, is shown in Figure 1. This behavior is indicative of ionic polarization. The initial current, however, varied linearly with applied voltage, exhibiting ohmic behavior and therefore this was utilized to obtain the total D.C. conductivity. The slope of the I-V curve yielded the conductance and the total conductivity was computed from the relation $\sigma = mL/A$ where m is the slope of the I-V curve, L is the thickness and A is the area of cross section of SiO_2. Because of the polarization, current reversal was not routinely carried out, but occasionally some measurements were obtained. The values thus obtained were found to be independent of the direction of the applied voltage.

Figures 2 - 5 show the typical current voltage plots at various temperatures. The behavior was ohmic at all the temperatures studied up to an applied emf of ~0.3 volts. Higher voltages resulted in considerable damage to the platinum electrodes and the sample, probably due to the formation of platinum silicide. In a few

experiments, macroscopic holes as large as 1.5 mm in diameter were found in the electrodes. For this reason, the applied voltages were restricted to 1 volt and platinum electrodes were replaced by tungsten electrodes.

Assuming that these cells are in thermal and chemical equilibrium, the measured conductivity corresponds to silica in equilibrium with the oxygen activity equivalent to the dissociation pressure of SiO_2-Si.

Figure 6 shows the Arrhenius plots for the total D.C. conductivity of SiO_2 grown on p-type and n-type silicon. Each plot clearly indicates two regions. Below ~450°C, the total conductivity is almost independent of temperature within the experimental scatter. Above ~450°C the conductivity rises sharply with temperature for SiO_2 grown on both p-type and n-type silicon. The activation energies were 1.65 eV and 2.10 eV for SiO_2 grown on p-type and n-type silicon, respectively.

The A.C. conductivity was measured in the temperature range of 500 - 1100°C initially at 1 kHz and subsequently at frequencies down to 50 Hz. Below 500°C, the conductivity was too low to be measured accurately by the conductivity bridge used. Figures 7 and 8 show the plots of $\log \sigma$ (1 kHz) vs. reciprocal of temperature in the temperature range 500 to 1100°C for SiO_2 grown on p-type and n-type silicon respectively. Both the plots yielded straight-lines. The activation energies calculated from the slopes of these lines were 1.55 eV and 1.86 eV for SiO_2 grown on p-type and n-type silicon respectively. Conductivity vs. frequency plots are shown in Figure 9

for various temperatures. The conductivity of SiO_2 grown on n-type silicon decreases above $1000^\circ C$. The values of A.C. conductivity at a fixed temperature were found to be higher than the D.C. conductivity. However, after extrapolating the A.C. conductivity data to zero frequency, the values, although slightly higher, were very close to the D.C. conductivity values. The variation of conductivity with frequency was more pronounced in the SiO_2 grown on p-type silicon than the one grown on n-type Si. An activation energy for conduction (extrapolated to zero frequency) of SiO_2 grown on p-type silicon was estimated to be 1.73 eV (Fig. 10). This is in close agreement to that obtained from the D.C. conductivity (1.65 eV).

Figure 11 shows the temperature dependence of A.C. conductivity at 1 kHz for different thicknesses of SiO_2. The conductivity values fall on a single straight line within experimental error, suggesting no dependence on oxide thickness. Figure 12 shows the Arrhenius plot for the conductivity of SiO_2 grown in wet oxygen. Analysis of this plot yields an activation energy of 1.2 eV. Comparison of this plot with that in Figure 7 shows that the conductivity for the wet oxide is higher than for the dry oxide.

Asymmetric cell B (Polarization measurements)

D.C. polarization measurements were made using an asymmetric polarization cell configuration B. In this type of cell, the ionic conduction is blocked due to application of positive potential on SiO_2/Pt side. Under these conditions, for a mixed conductor a steady state current (I) for a given applied potential (V) is given by the following expressions [13, 14].

$$I = -\frac{AkT}{Le} \sigma_n [1 - \exp(-eV/z_i kT)] + \sigma_p [\exp(eV/z_i kT) - 1] \qquad (1)$$

where A is the cross-sectional area, L is the thickness of the SiO_2 sample, e is the electronic charge, z_i, is the effective charge on an oxygen ion and σ_n and σ_p are the electronic conductivities due to electrons and holes respectively. In the limiting case when $V \gg kT/e$

$$I = -\frac{AkT}{Le} [\sigma_n + \sigma_p \exp eV/kT] \qquad (2)$$

thus the plot of I vs. $\exp eV/z_i kT$ yields a straight line. The slope and the intercept of this line gives σ_p and σ_n respectively.

$$\sigma_n = \frac{Le}{AkT} \text{ (intercept extrapolation of plateau)}$$

$$\sigma_p = \frac{Le}{AkT} \text{ (slope)}$$

Moreover, the shape of the current vs. polarization potential is indicative of the n or p character of the material [13].

Figures 13 - 16 show the current voltage plots for SiO_2 grown on n- and p-type silicon in the temperature range 545°C to 960°C. These plots show a plateau indicating that the electronic conductivity is predominantly due to electrons. The partial conductivity due to electrons can be obtained from the extrapolation to zero applied voltages of the plateau in the above curves. The electronic transference number estimated from the partial electronic conductivity and total conductivity for SiO_2 grown on n-type substrate is found to be higher than for SiO_2 grown on p-type at higher temperatures. An Arrhenius plot for the conductivity due to the electrons is shown in Figure 17.

Asymmetrical cell B (Open circuit voltage measurement)

Open circuit voltage measurements were made using Cell B. In these measurements the oxygen activity varied on one side using Ar + O_2

mixtures while oxygen activity at the other side was fixed by the Si -
SiO_2 equilibrium.

The emf of this cell is given by,

$$E_{theoretaical} = \frac{RT}{nF} \ln \frac{PO_2 \text{ (in argon)}}{PO_2 \text{ (Si/SiO}_2)}$$

and

$$t_i = \frac{E_{measured}}{E_{theoretical}}$$

where E is emf in volts, $E_{theoretical}$ is that calculated from the
free energy of formation, F is Faraday, n is number of electrons per
mole of oxygen involved in the transport. The partial
pressure of oxygen in argon was controlled by passing argon over
titanium chips kept at different temperatures. For higher oxygen
pressures pure Ar and oxygen were mixed in desired proportions. The
oxygen pressures were measured using a zirconia probe. Figure 18
shows the plot of log PO_2 vs. FE/2.303 RT. The slope of this plot
yields t_i/n' over a given pressure range. The t_i for SiO_2 grown on
n-type Si was calculated assuming n = 4 per mole of oxygen and was
found to vary from 0.4 at low oxygen pressure to 0.76. These data are
consistant with the observations made by Mills and Kroger [11].

The data obtained in the present investigation are compared with
the data reported by other investigators in Figure 19. It is clearly
evident that below a certain critical temperature, the total
conductivity is almost independent of temperature and above this
temperature the conductivity increases in temperature with a higher
activation energy. There is considerable discrepancy between various
investigators regarding the temperature at which this transition
occurs. Our data shows a comparatively sharper transition. The

temperature independent conductivity below 450°C for our data is likely to be due to electronic contribution and is thought to be impurity controlled. Conduction in the higher temperature range from 450 to 960°C is mixed ionic and electronic.

Table 1, shows the available experimental, theoretical and extrapolated conductivity data at 850°C and 25°C and in Table 2, the corresponding activation energies have been summarized. The values of conductivity at 850°C calculated by Raleigh [10] from two independent approaches are $3.7 \times 10^{-11} \text{ohm}^{-1}\text{cm}^{-1}$ and $3.5 \times 10^{-11}\text{ohm}^{-1}\text{cm}^{-1}$. The former value is obtained from the experimental data of Jorgensen [6] whereas the latter value was estimated from the diffusion of oxygen in SiO_2 as measured by Sucov [2]. These values may be compared with our D.C. conductivity values viz $10 \times 10^{-11} \text{ohm}^{-1}\text{cm}^{-1}$ and $8 \times 10^{-11}\text{ohm}^{-1} \text{cm}^{-1}$ for SiO_2 grown on p-type and n-type silicon, respectively.

Our D.C. conductivity data obtained for different thickness of SiO_2 are reproducible within an error limit of 30 - 40% and are in good agreement with Raleigh's [10] calculated values. The absolute values of conductivity differ by 50 - 60%, which is reasonable for such a highly insulating material. The extrapolated data of Tripp, et al. [12] differ from our D.C. values by two orders of magnitude while their data agree reasonably well with our A.C. values. The value of conductivity reported by Mills and Kroger [11] is greater by 4 - 5 orders of magnitude as compared to our D.C. values and 3 orders of magnitude as compared to our A.C. values.

To separate out the electronic conductivity from the total conductivity we chose the D.C. total conductivity values. As

discussed earlier, the A.C. conductivity values extrapolated to zero frequency are higher than D.C. conductivity values. This may be because of the contribution of the dielectic loss due to variation in the capacitance with frequency and temperature. The high conductivity of SiO_2 grown in wet oxygen conditions is suggested to be due to the presence of appreciable amount of OH [18] and probably more nonbridging oxygen [19].

Examination of the activation energy data reported in Table 2, reveals that our data agrees closely with that of Law [16] who has obtained an activation energy value of 1.57 eV from oxidation data assuming the parabolic rate law. He suggested that this represents the energy of the transport of ions during thermal oxidation of silicon.

Considering only the electronic conductivity obtained from the measurements on the asymmetric cell, the activation energy is estimated to be 2.7 eV above ~700°C (See Figure 17). Conductivity due to electrons is lower than that due to ions by more than one order of magnitude. Further evidence of mixed conductivity is found from the results obtained from polarization measurements. From the total conductivity data, and the electronic conductivity data, ionic conductivity values were determined for different temperatures. The percentage of ionic conductivity has been plotted as a function of temperature in Figure 20. As shown in this figure, the ionic conductivity is only 40% at 545°C, and rises with temperature to a maximum of ~95% in the case of SiO_2 on p-type silicon, and ~86% for SiO_2 grown on n-type silicon between 700°C to 875°C. Above this

temperature, the values drop steeply. The decrease in the A.C. conductivity of SiO_2 on n-type silicon above $1000^{\circ}C$ suggests that either the charge carriers experience some kind of repulsive effect in SiO_2, or that some kind of trapping of charges occur at the Si/SiO_2 interface.

The above data suggest that conduction in SiO_2 at an oxygen pressure corresponding to Si/SiO_2 equilibrium and at temperatures above 450°C, takes place via charged oxygen species as well as electrons. Transport via charged oxygen species is likely to be either because of the presence of oxygen interstitials at higher oxygen pressures or due to oxygen vacancies at lower oxygen pressures. Since the oxygen pressures surrounding SiO_2 in our investigations is very low (Si/SiO_2 equilibria), the latter seems to be more favorable. Oxygen vacancies can be generated according to the following defect equilibrium:

$$Oo = 1/2 \ O_2 + V\ddot{o} + 2e$$
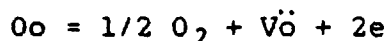
hence

$$K = [V\ddot{o}] \ [e']^2 P_{O_2}$$

Thus, the effect of the decrease in oxygen pressure would be to increase the electronic as well as the ionic conductivity. In SiO_2 the electronic conductivity is mainly due to electrons. At temperatures below $450^{\circ}C$ the electrons, which are generated with increase in temperature, either pair with holes or are being trapped by the impurities, hence the electronic conductivity in this temperature range does not increase significantly. The above defect mechanism is in agreement with the experiments made by Folkes, et al. [17]. The

above equilibrium will be strongly influenced by the presence of aliovalent impurities. It has been suggested in the literature that during oxidation of silicon doped with B or P, the oxide contains detectable amounts of B or P as a result of redistribution of impurities. Segregation coefficient suggests the incorporation of boron into SiO_2 while rejection of the phosphorous back into the silicon [20]. The presence of B or P would affect the above equilibrium. If the trivalent boron dissolves substitutionally into the SiO_2 lattice, additional oxygen vacancies would be generated to satisfy the condition of electroneutrality. On the other hand the number of oxygen ion vacancies would be decreased because of the presence of pentavalent phosphorous ions in the cation lattice.

The higher values of conductivities of SiO_2 grown on silicon containing B, as compared to those containing P, seems consistent with the increased concentration of oxygen vacancies due to such a mechanism during the transport through SiO_2 in this oxygen pressure range.

At high oxygen pressures however, presence of oxygen inter-stitials is more likely. The presence of pentavalent phosphorous will then increase the number of interstitial oxygen ions and the holes associated with it while boron will have the opposite effect. Our measurements on the oxidation of silicon in 1 atm of oxygen (unpublished) show that phosphorous doped silicon oxidises faster than boron doped silicon suggesting the presence of intestitial silicon and holes at this oxygen pressure.

The transport number measurements show that the ionic trans-

ference number is a function of oxygen pressure and temperature. There appears to be a critical oxygen pressure at which a switchover of the predominant defect from oxygen interstials to oxygen vacancies may occur. This can only be resolved by measuring the conductivities as a function of oxygen pressures over a wider pressure range.

ACKNOWLEDGEMENTS

REFERENCES

[1] F.J. Norton, Nature $\underline{181}$ 701 (1961).

[2] E.W. Sucov, J. Am. Ceram. Soc. $\underline{46}$ 14 (1963).

[3] E.A. Irene, J. Elec. Soc. $\underline{129}$, 413, 1982.

[4] J.R. Ligenze and W.G. Spitzer,. J. Phys. Chem. Solids $\underline{14}$ 131 (1960).

[5] W.A. Pliskin and R.P. Gnall, J. Electro. Chem. Soc. $\underline{111}$ 872 (1964).

[6] P.J. Jorgensen, J. Chem. Phys. $\underline{37}$ 874 (1962).

[7] A.G. Revesz, J. NonCrystalline Solids $\underline{4}$ 347 (1970).

[8] A.G. Revesz and R.J. Evans, J. Phys. Chem. Solids $\underline{30}$ 551 (1966).

[9] L. Pauling, J. Phys. Chem. $\underline{56}$ 361 (1962).

[10] D.O. Raleigh, J. Electrochem. Soc. $\underline{113}$ 782 (1966).

[11] T. Mills and F.A. Kroger, J. Electrochem. Soc. $\underline{120}$ 1582 (1973).

[12] W.C. Tripp, et al., J. Final Report ARL TR75-0130 June 1975.

[13] C. Wagner, Int. Com. of Electrochem., Thermodynamics and Kinetics, Proc. 7th Meeting, Lindau 1955.

[14] J.B. Wagner, Jr. and C. Wagner, J. Chem. Phys. $\underline{26}$ 1597 (1957).

[15] H.F. Wolf, Silicon Data Handbook, Pergamon Press (1969).

[16] J.T. Law, J. Phys. Chem. $\underline{61}$ 1200 (1957).

[17] F.M. Folkes, Abstract No. 166 Electro. Chem. Soc. Meeting., St. Louis, Missouri, May 6-11, 1980.

[18] R. Pfeffer and M. Ohring, J. Appl. Phys. $\underline{52}$, 777 (1981).

[19] S.K. Ghandhi, "The Theory and Practice of Microelectronics," John Wiley and Sons, Inc., 140, 1968.

[20] D.R. Lamb, Thin Solid Films, $\underline{5}$, 247, 1970.

[21] B.E. Deal and A.S. Grove, J. Appl. Phys. $\underline{36}$, 3770, 1965.

FIGURE CAPTIONS

Figure 1   Typical current vs. time curve at $860°C$ for SiO_2 grown on n-type Si in Cell A.

Figure 2   I-V curves for Cell A consisting of SiO_2 on p-type Si.

Figure 3   I-V curves for Cell A consisting of SiO_2 on p-type Si.

Figure 4   I-V curves for Cell A consisting of SiO_2 on n-type Si.

Figure 5   I-V curves for Cell A consisting of SiO_2 on n-type Si.

Figure 6   Log σ vs. reciprocal temperature for Cell A (SiO_2 on p-type Si; SiO_2 on n-type Si.

Figure 7   Log σ vs. reciprocal temperature for SiO_2 on p-type Si measured in Cell A (A.C. measurement 1 kHz).

Figure 8   Log σ vs. $10^3/T$ for SiO_2 on n-type Si measured in Cell A (A.C. measurements 1 kHz).

Figure 9 σ vs. frequency for SiO_2 on p-type Si in Cell A (solid line); and n-type Si (dashed line).

Figure 10   Log σ vs. $10^3/T$ for the data of Figure 9 extrapolated to zero frequency.

Figure 11   Conductivity vs. reciprocal temperature for different thicknesses of SiO_2 on p-type Si Cell A (A.C. measurement 1 kHz).

Figure 12   Log σ vs. reciprocal temperature for SiO_2 grown under wet condition on p-type Si Cell A (A.C. measurement 1 kHz).

Figure 13   Typical polarization curves for asymmetric Cell B containing SiO_2 on p-type Si.

Figure 14   Typical polarization curves for asymmetric Cell B containing SiO_2 grown on p-type Si.

Figure 15   Typical polarization curves for asymmetric Cell B containing SiO_2 grown on n-type Si.

Figure 16   Typical polarization curve for asymmetric Cell B containing SiO_2 grown on n-type Si.

Figure 17   Log σ_n vs. $10^3/T$ for SiO_2 on p-type Si substrate.

TABLE 1

CONDUCTIVITY DATA

References		Conductivity ohm^1 Cm^1 850 °C	25 °C
Jorgensen [6] & Raleigh [10]	(a)	3.7×10^{-11}	
Sucov [2] & Raleigh [10]	(b)	3.5×10^{-11}	
Tripp, et al. [12]	(c)	8.9×10^{-8}	
Mill & Kroger [11]	(d)	6.3×10^{-6}	1.65×10^{-10}
Brander, et al. [15]	(e)		1.70×10^{-11}
Wolf [15]	(f)		3.3×10^{-16} 5×10^{-17}
Present work 　D.C. Measurement		SiO_2 on p-type Si 10×10^{-11} SiO_2 on n-type Si 7.8×10^{-11}	5.0×10^{-16} 2.75×10^{-16}
A.C. Measurement		SiO_2 on p-type Si 10×10^{-9} SiO_2 on n-type Si 3.16×10^{-9}	
Extrapolated to 　zero frequency		SiO_2 on p-type Si 6×10^{-10}	

(a) Calculated by Raleigh [10] from Jorgensen's data [6]
(b) Calculated by Raleigh [10] from Sucov's data [2]
(c) Extrapolated from the data of Tripp, et al. [12]
(d) Extrapolated from Mills and Kroger data to 850°C
(e) Extrapolated to 25°C
(f) Data from Silicon handbook [15]

TABLE 2

ACTIVATION ENERGY (eV)

References	Temp. Range °C	From Conductivity	From Diffusion	From Rate Constant	
Tripp, et al [12]	1300-1400 1400-1550	0.72 2.93		(a)	(b)
Mills & Kroger [11]	400- 600	1.20			
Norton [1]	950-1100		1.17		
Sucov [2]	925-1225		3.08		
Deal [21]				1.29	2.05
Law [16]	727-1027			1.57	0.90
Present work	500- 960 500- 960 550-1100 550-1000 550-1000 550-1000	1.65 (c) 2.10 (d) 1.55 (e) 1.86 (f) 1.73 (g) 1.20 (h)			

(a) From parabolic rate law
(b) From linear rate law
(c) For SiO_2 grown on p-type Si (D.C. measurement)
(d) For SiO_2 grown on n-type (D.C. measurement)
(e) For SiO_2 grown on p-type Si (A.C. measurement 1 kHz)
(f) For SiO_2 grown on n-type Si (A.C. measurement 1 kHz)
(g) For SiO_2 grown on p-type (A.C. measurement extrapolated to zero frequency)
(h) For SiO_2 grown on p-type under wet conditions (A.C. measurements 1 kHz)
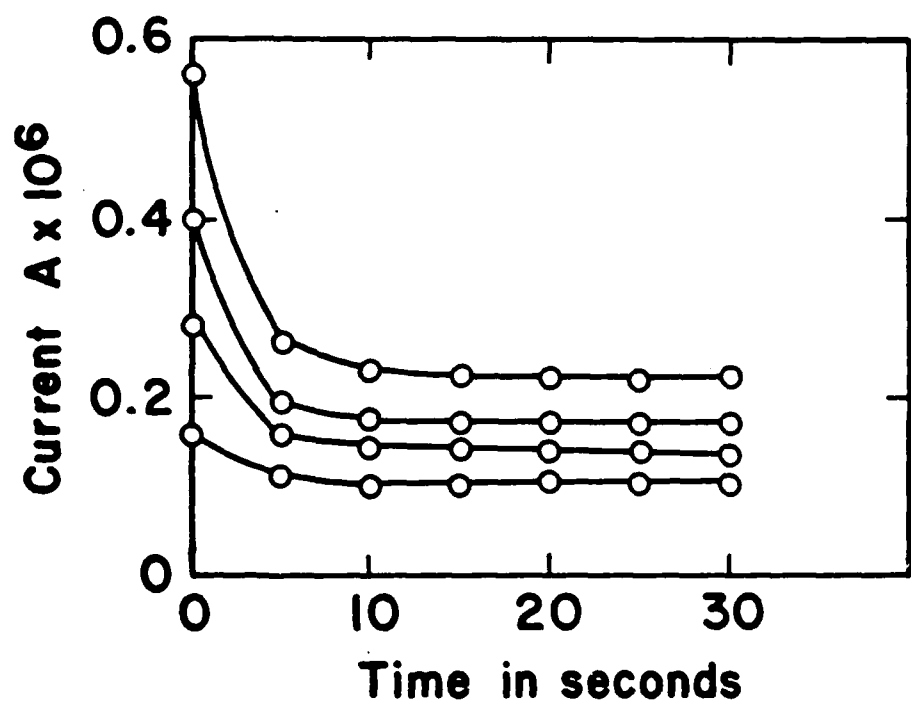
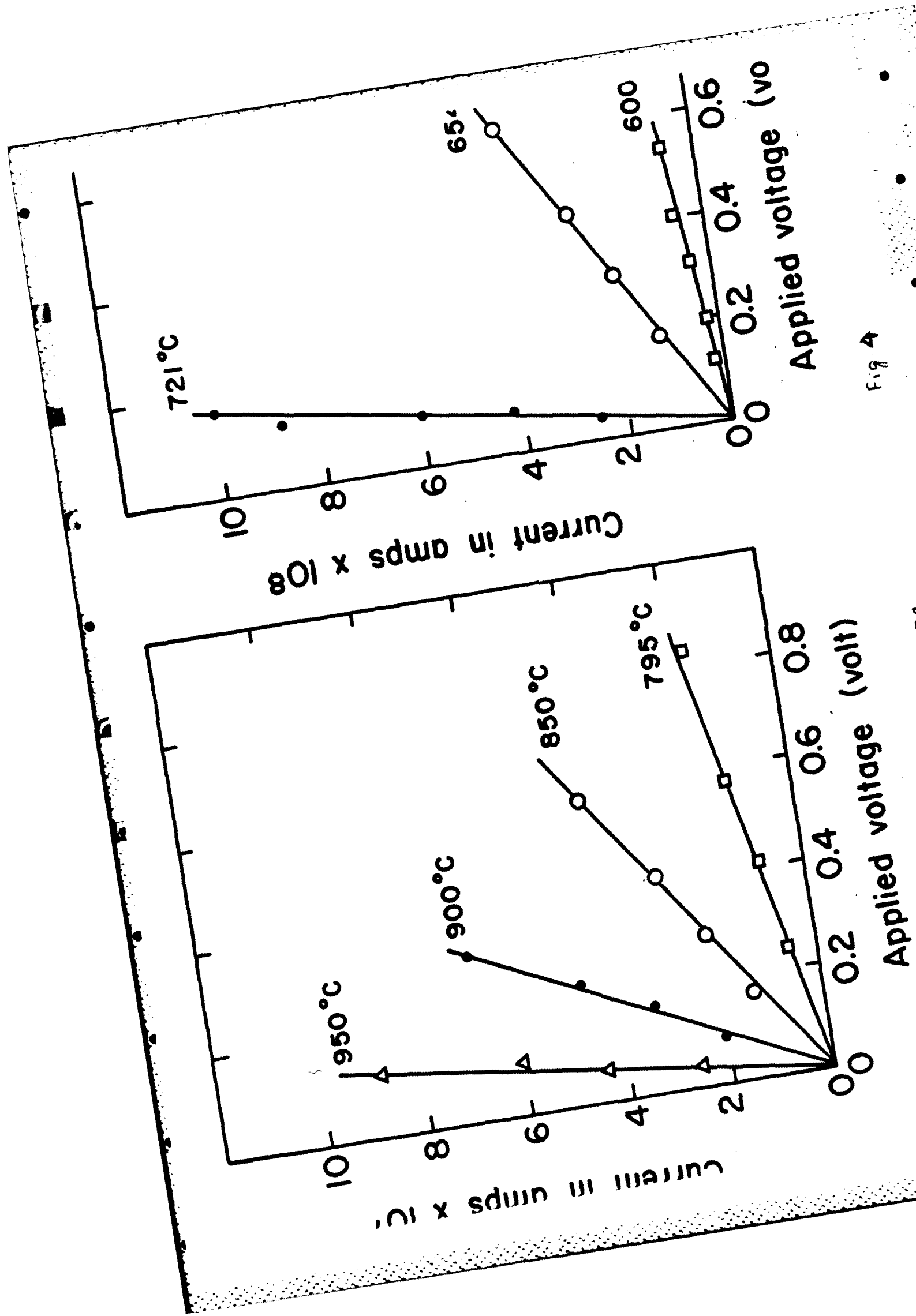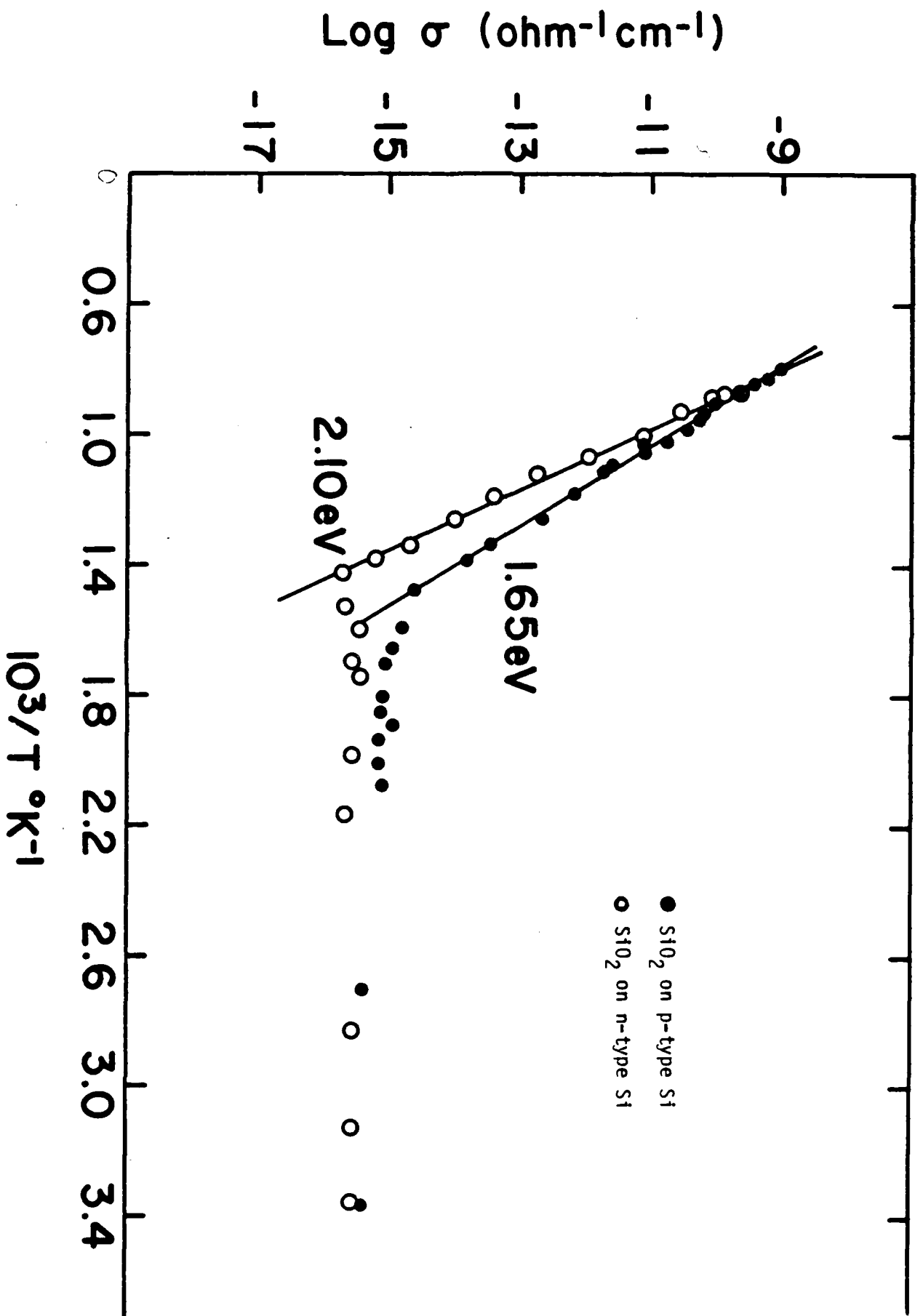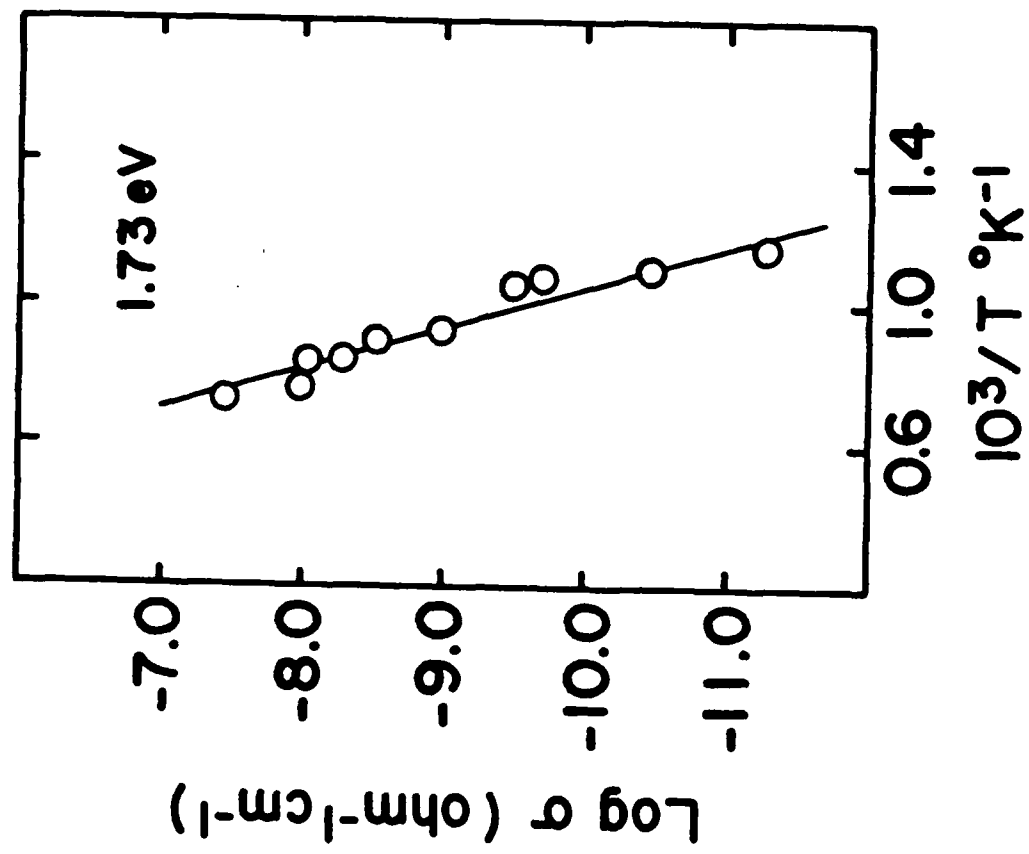Fig. 1   SRIVASTAVA, PRASAD, WAGNER
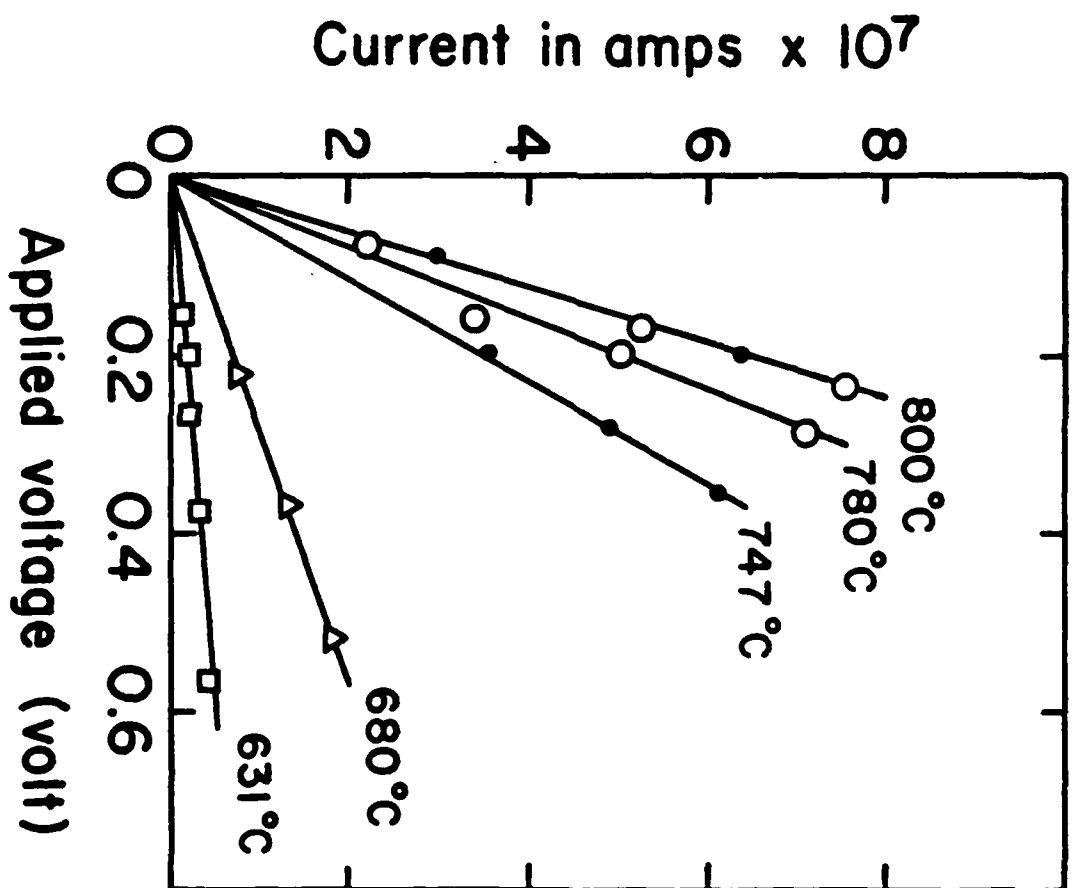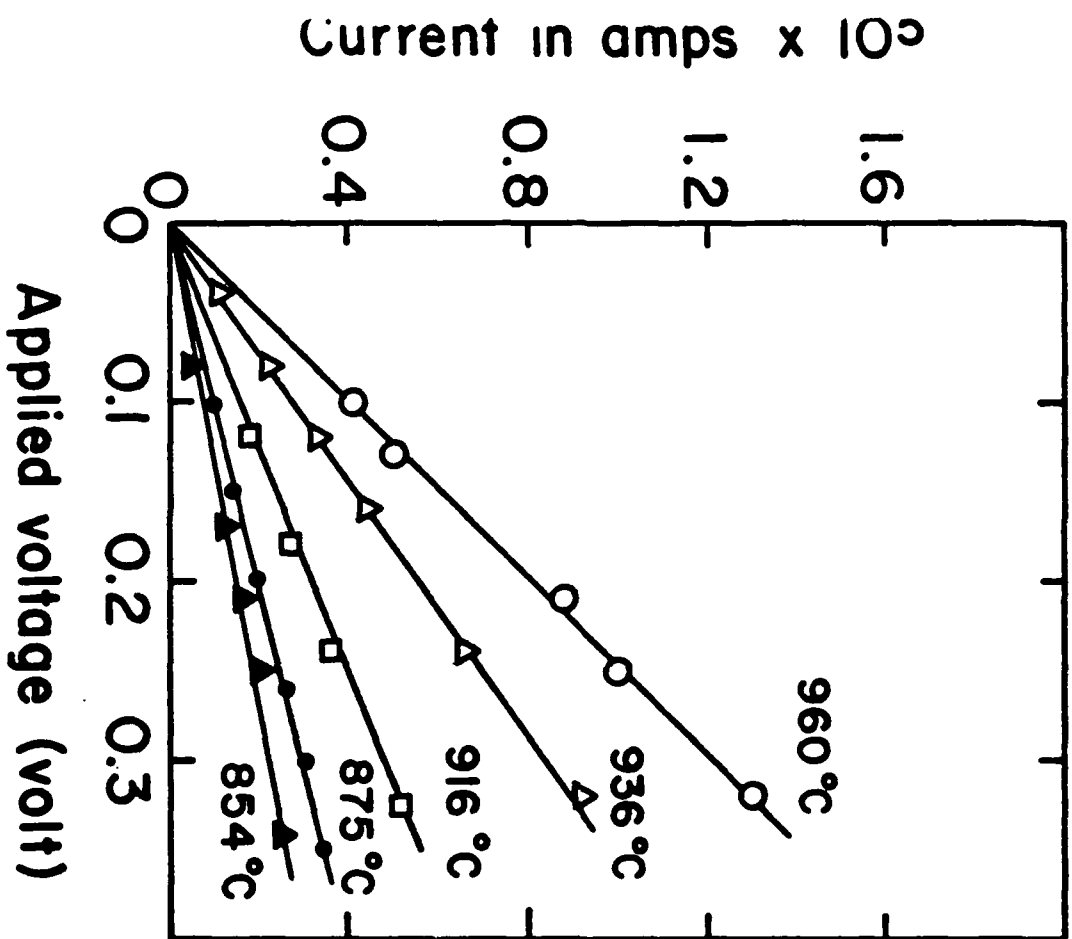
Fig 3

SRIVASTAVA   PRASAD , WAGNER
[3]
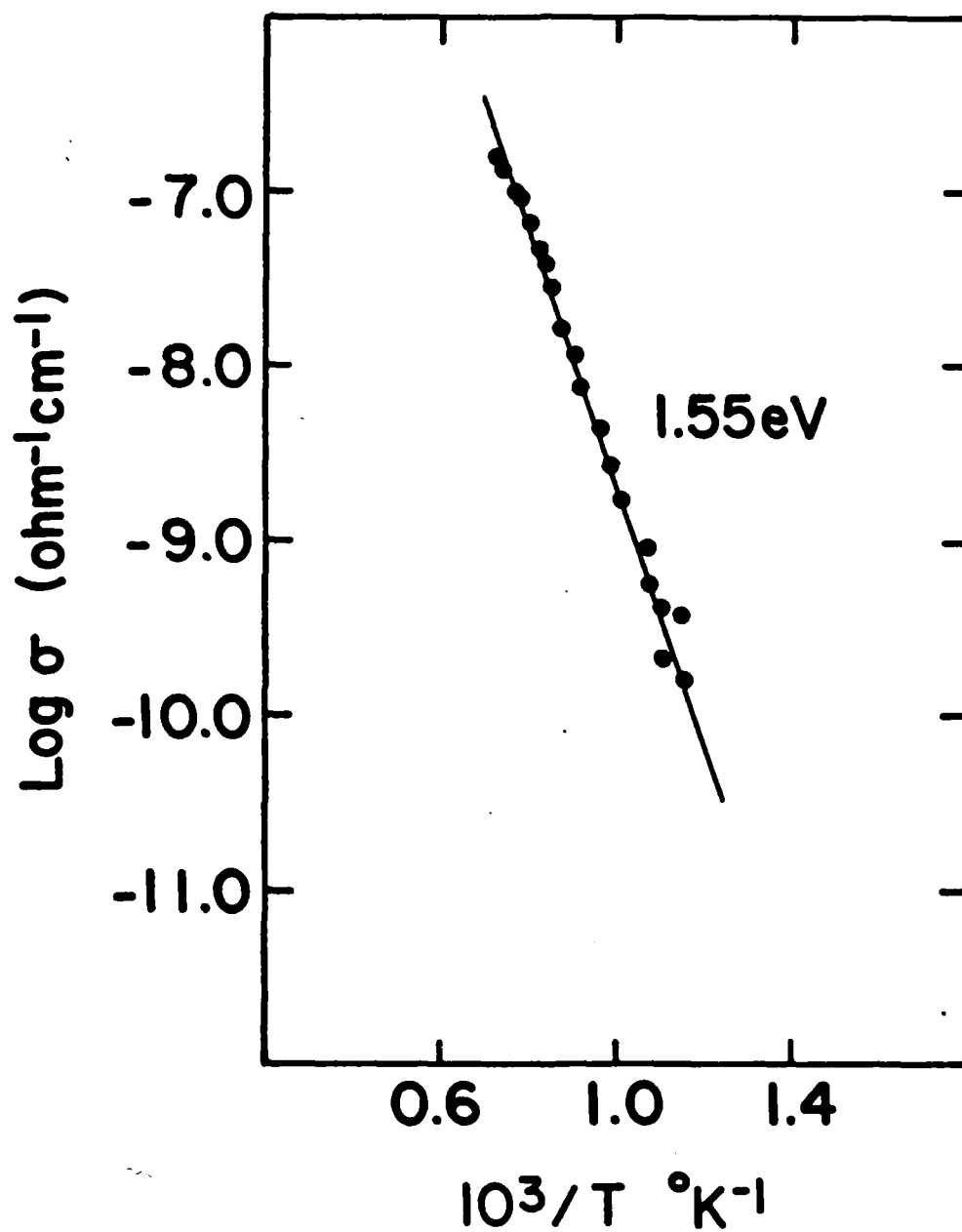
Fig 2

Fig 4

Current in amps x 10⁸

Applied voltage (vo

721°C

65‹

600

600

0   0.2   0.4   0.6

Fig 5   SRIVASTAVA · PRASAD   WAGNER

Current in amps x 10'

Applied voltage (volt)

950°C

900°C

850°C

795°C

0   0.2   0.4   0.6   0.8

Fig 6

Log σ (ohm⁻¹cm⁻¹)

Axis labels: Log σ (ohm^{-1}cm^{-1}) with values -17, -15, -13, -11, -9

X-axis: $10^3/T$ °K^{-1} with values 0.6, 1.0, 1.4, 1.8, 2.2, 2.6, 3.0, 3.4

2.10eV

1.65eV

● SiO₂ on p-type Si
○ SiO₂ on n-type Si

Fig 7

SRIVASTAVA, PRASAD, WAGNER

Fig. 8   SRIVASTAVA, PRASAD, WAGNER

1.86eV

$10^3/T°K^{-1}$

Log σ (ohm⁻¹cm⁻¹)

Fig 9

Frequency in Hz

Conductivity (ohm⁻¹ cm⁻¹)

1050°C
960°C
940°C
918°C
862°C
830°C
837°C
740°C
665°C
600°C
600°C

SRIVASTAVA, PRASAD, WAGNER

Fig. 10

SRIVASTAVA, PRASAD, WAGNER

Conductivity (ohm⁻¹cm⁻¹) vs $10^3/T \ ^\circ K^{-1}$

Legend:
- 6KA°
- ▲ 9KA°
- ○ 10KA°
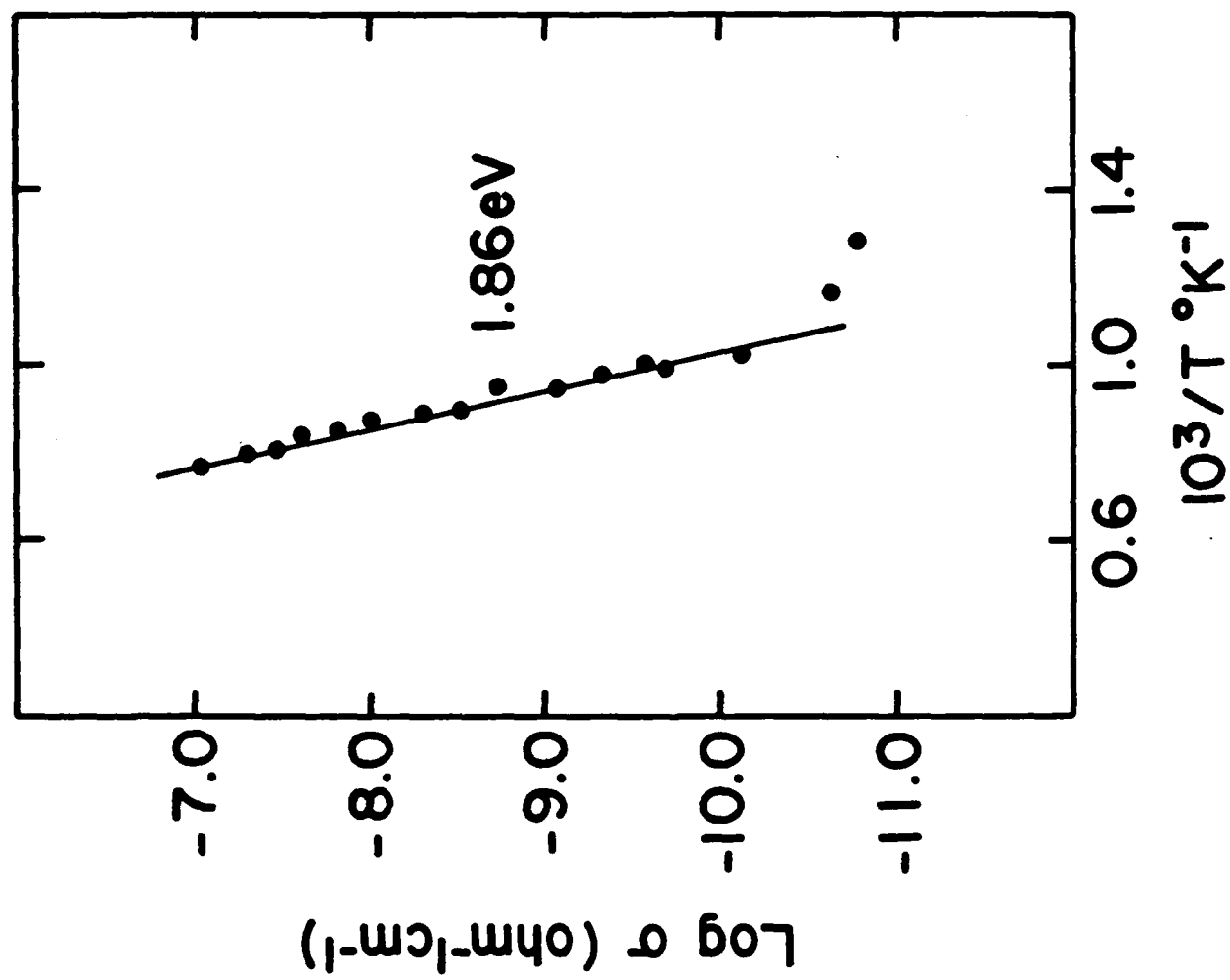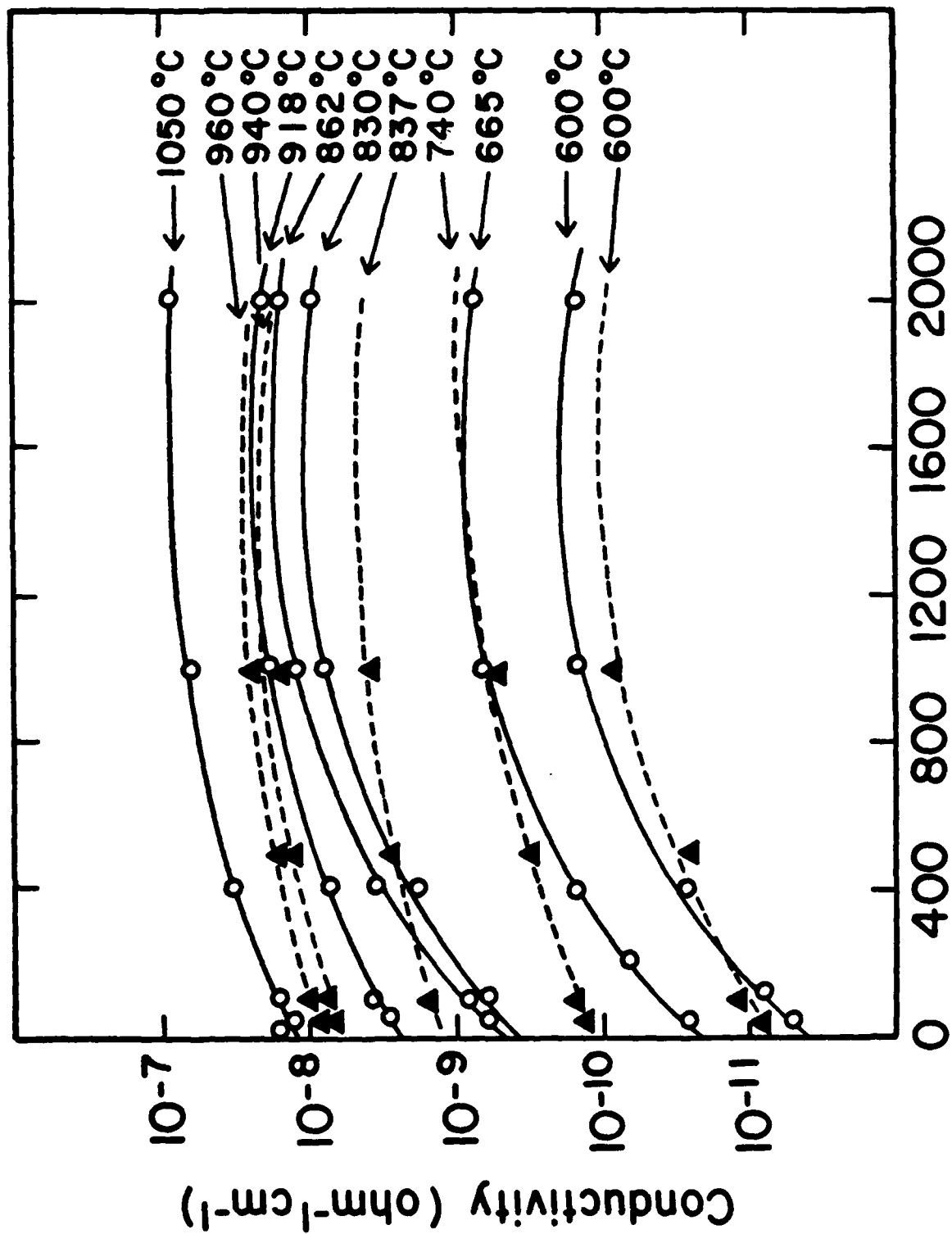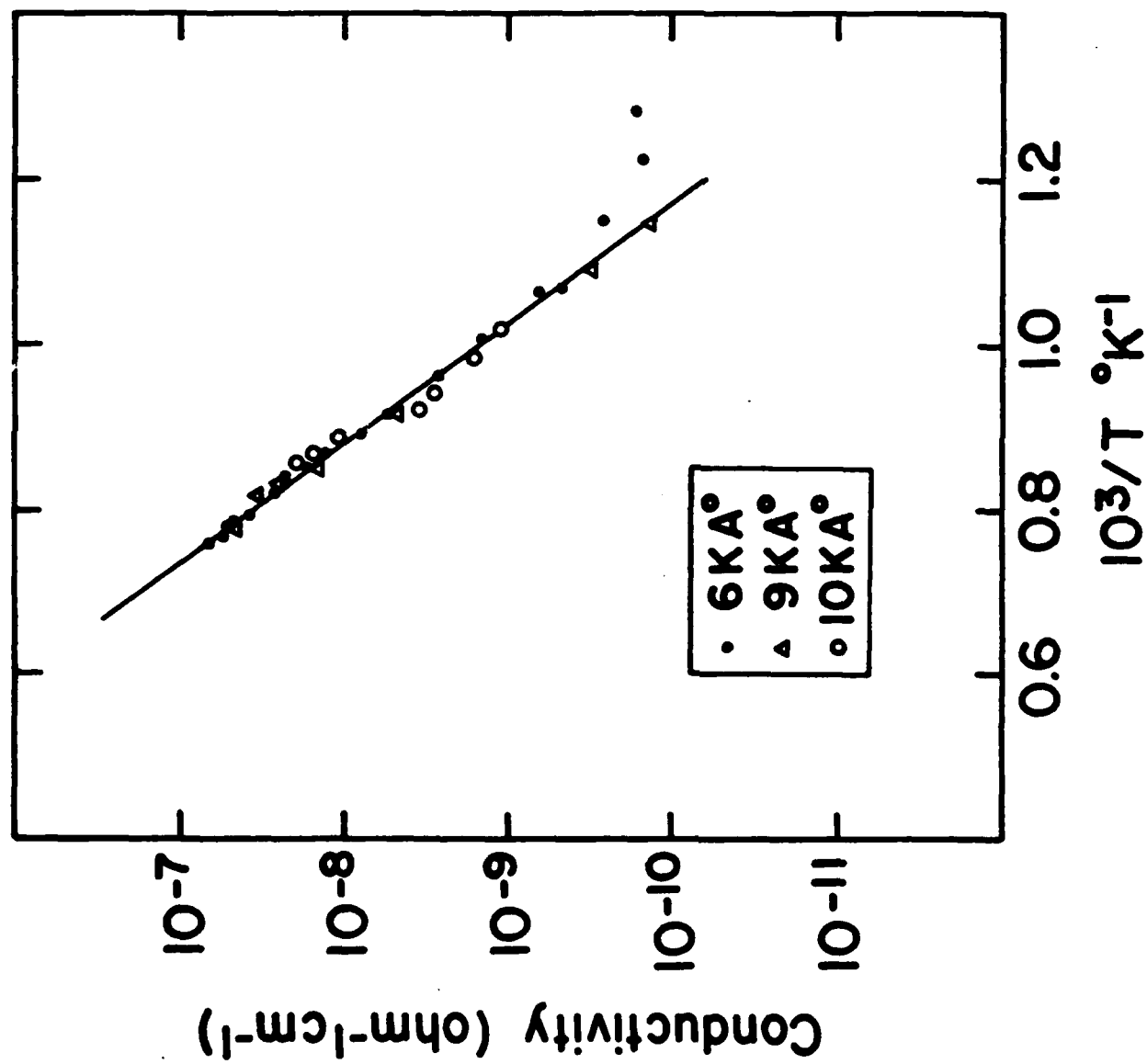
Fig. 11

SRIVASTAVA , PRASAD , WAGNER

Fig 12   SRIVASTAVA, PRASAD, WAGNER

Polarization potential (Volt)

I (Amps)

914°C

843°C

781°C
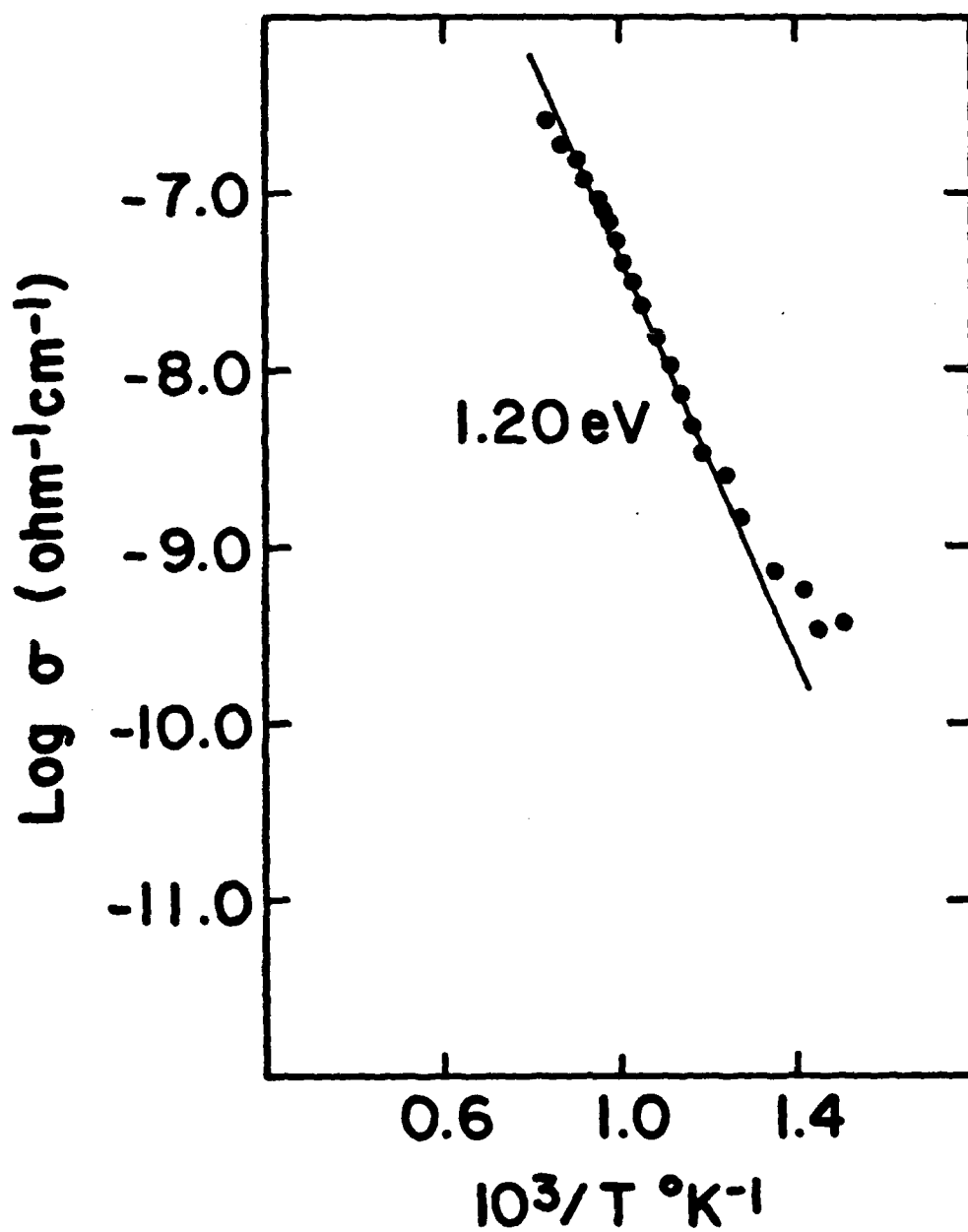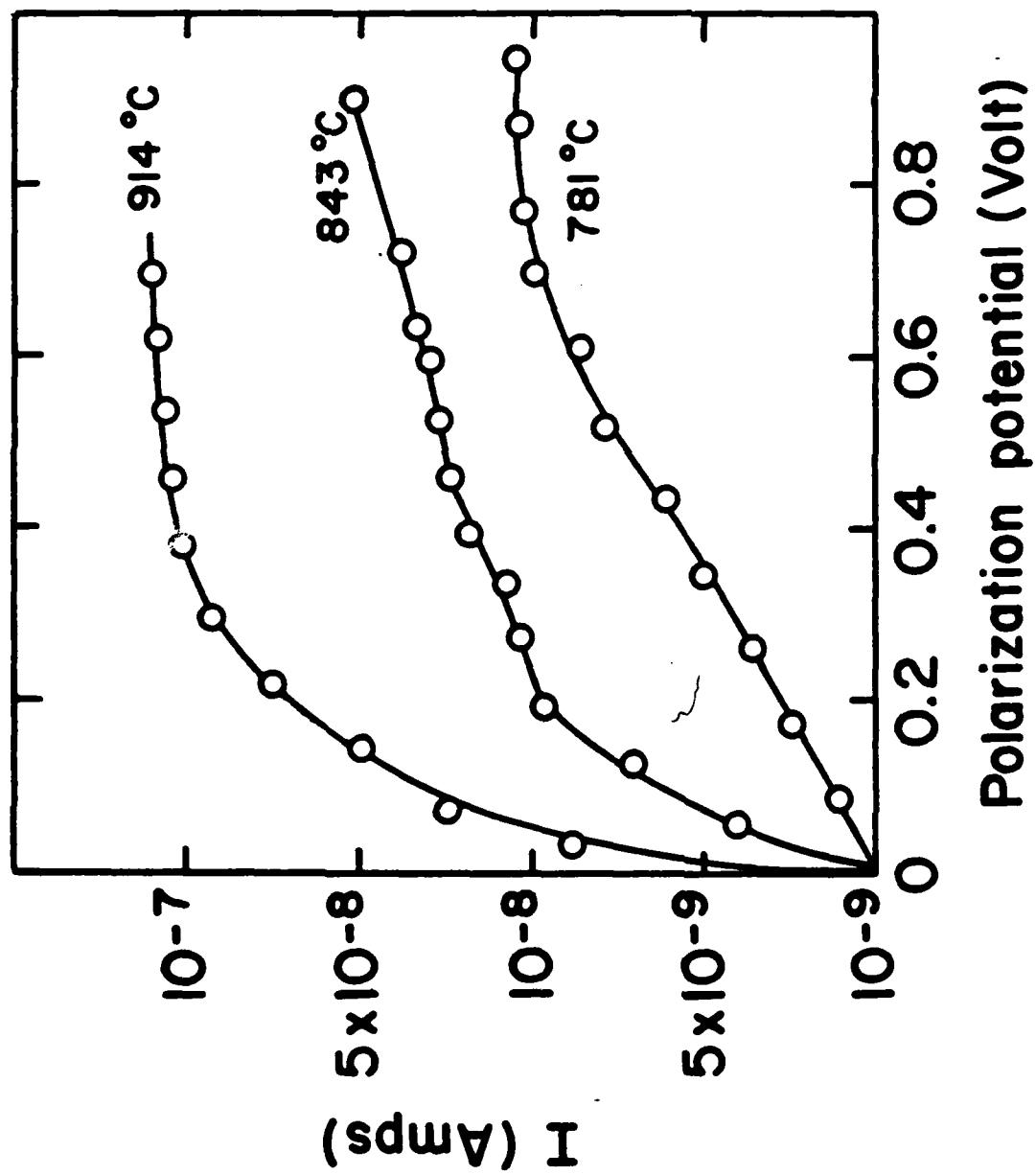
Fig. 14

SRIVASTAVA, PRASAD, WAGNER

Fig 13

SRIVASTAVA, PRASAD, WAGNER

I (Amps)

Polarization potential (Volt)

727°C

670°C

561°C
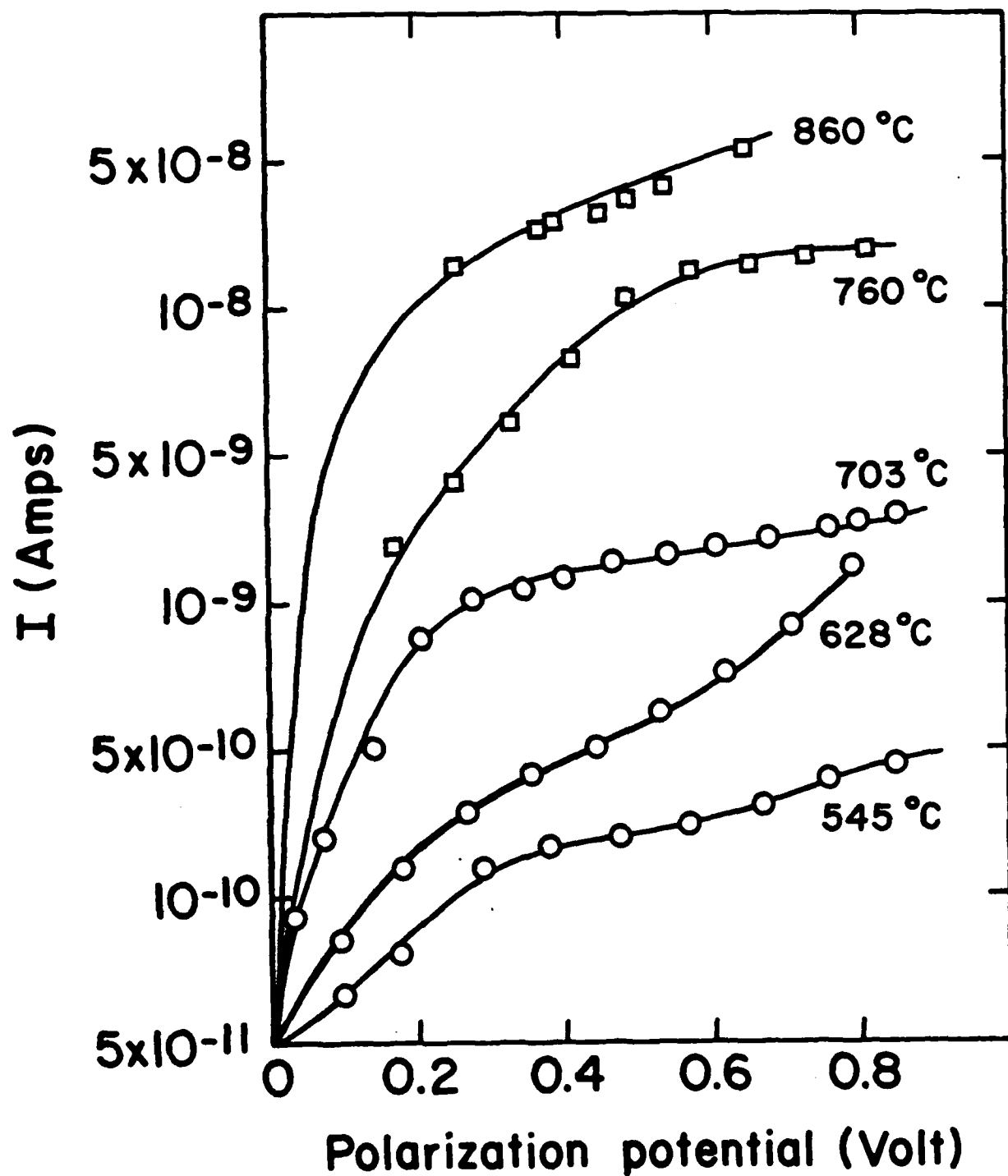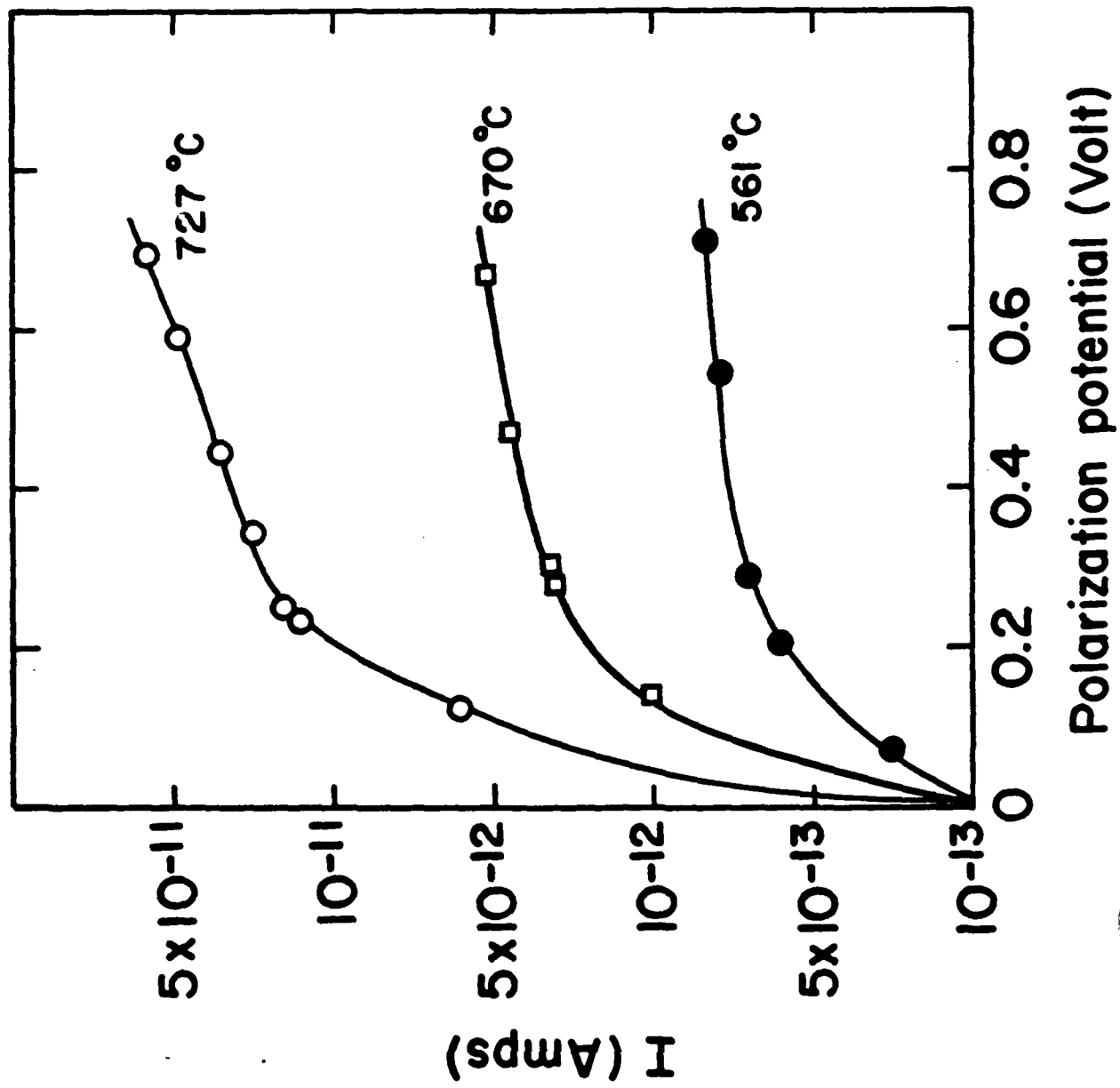
SRIVASTAVA , PRASAD , WAGNER

Fig 15

Fig 16

SRIVASTAVA, PRASAD, WAGNER
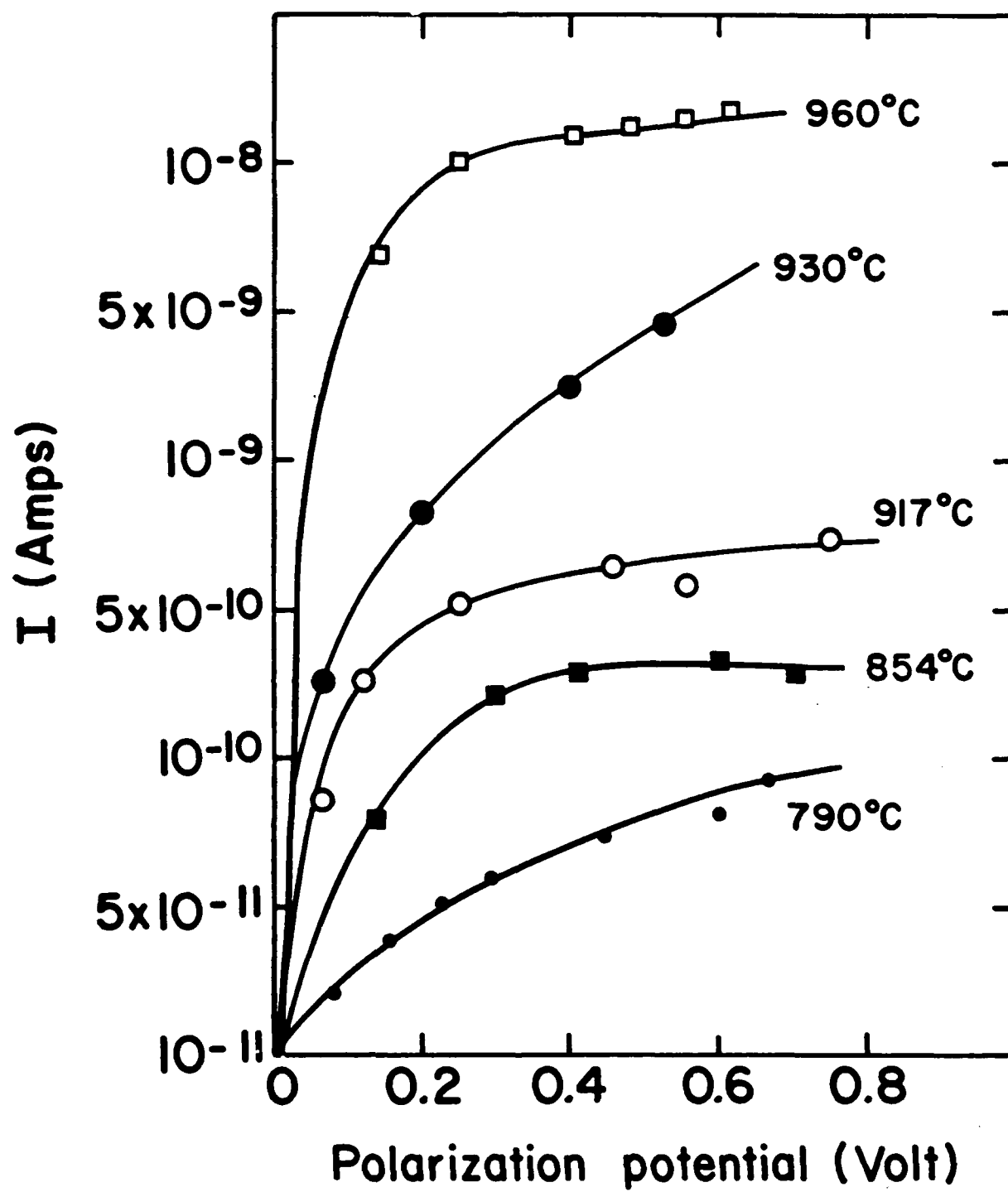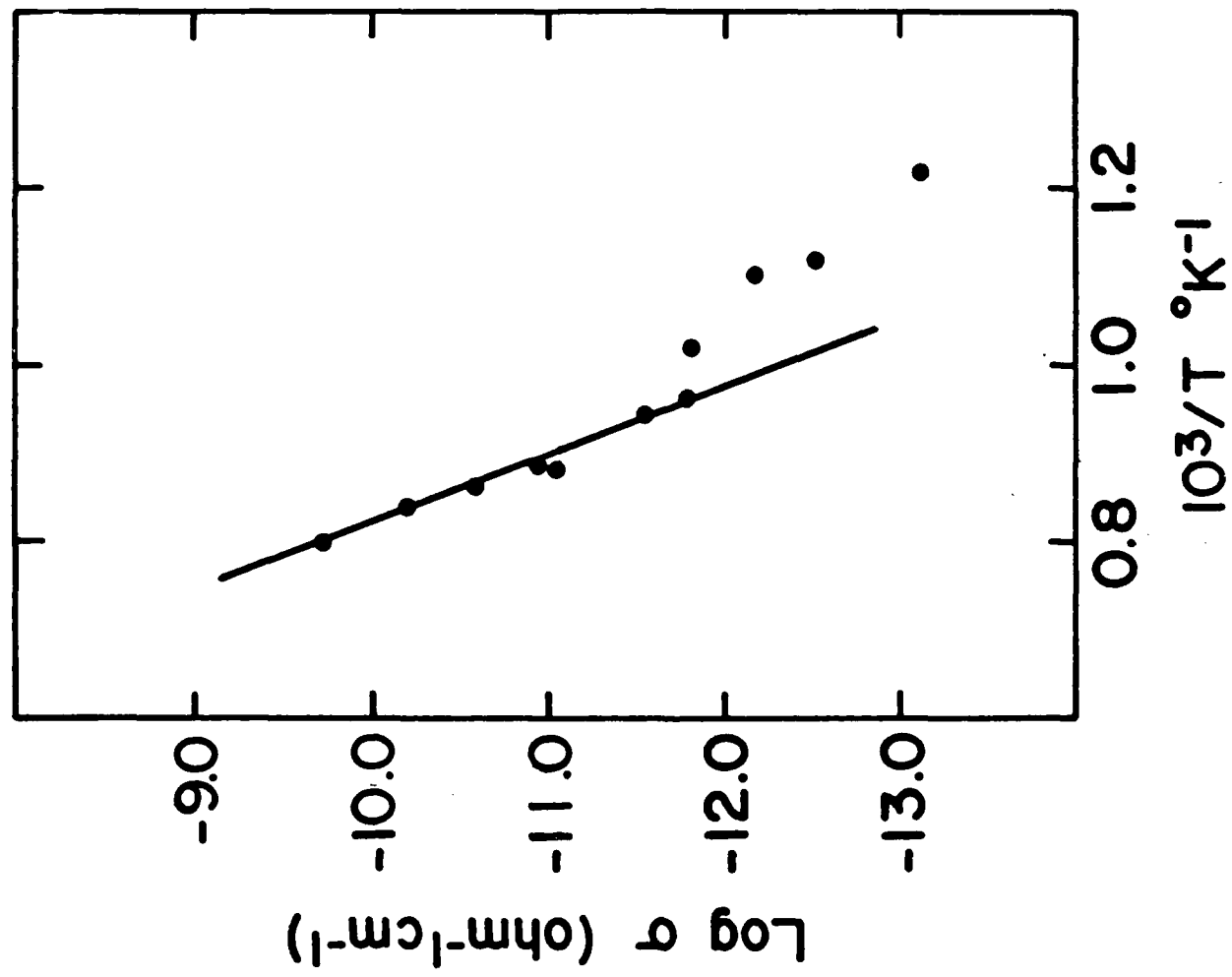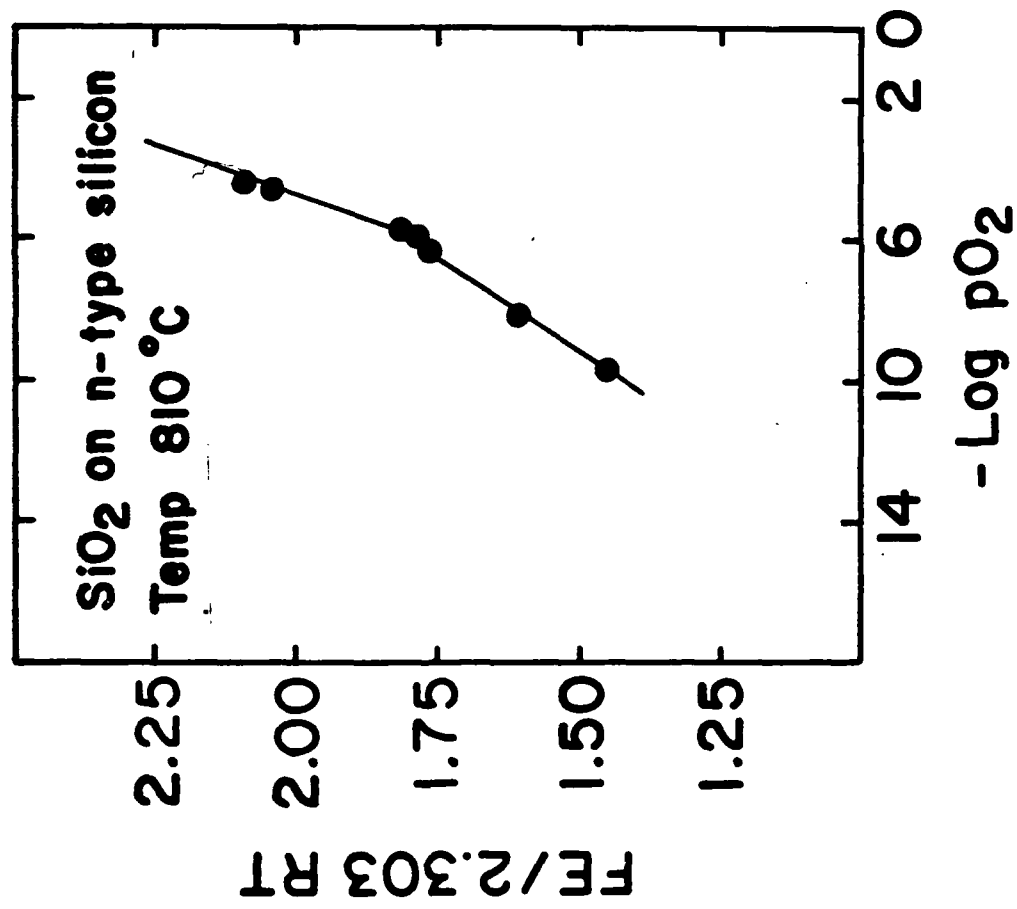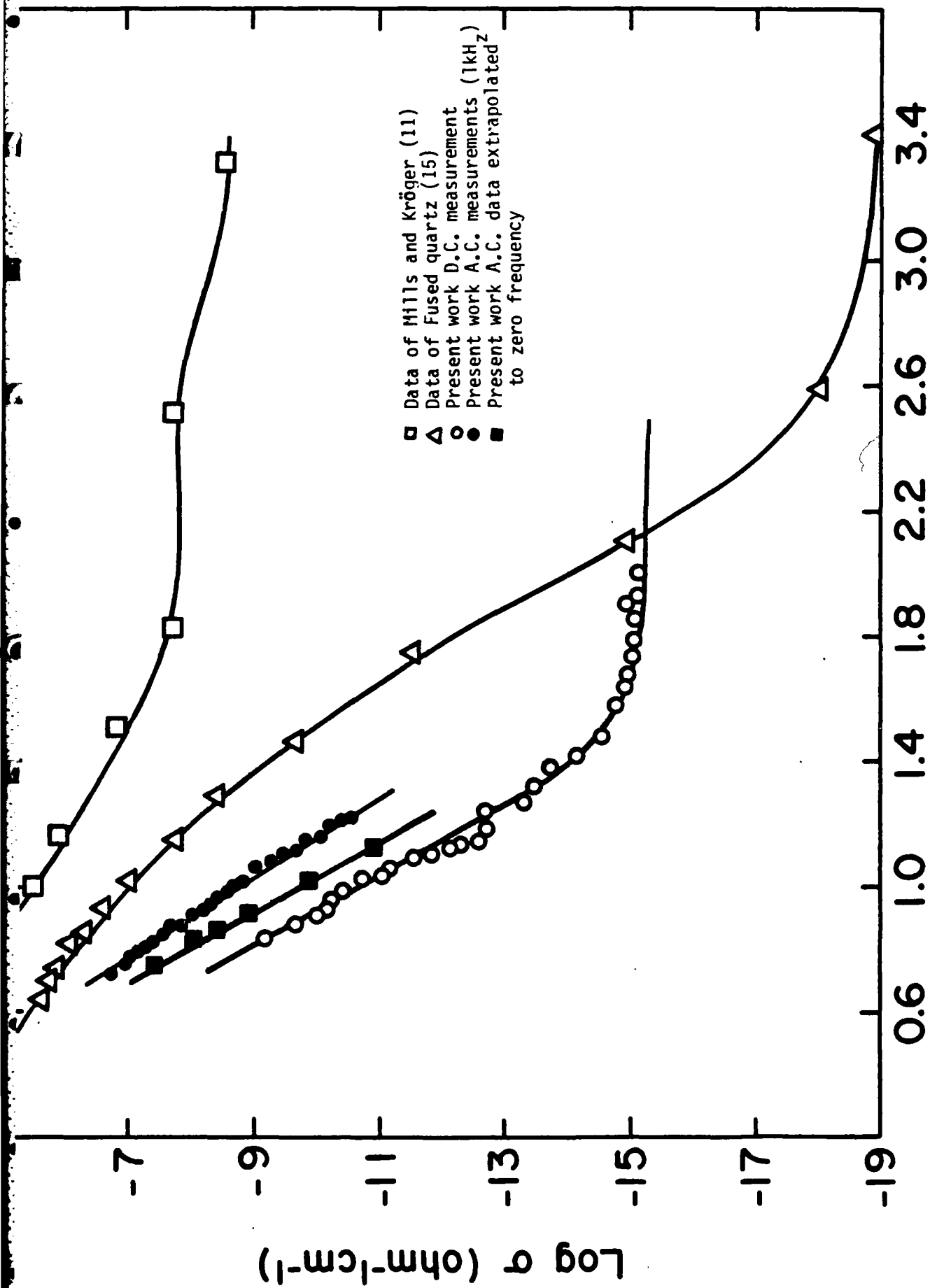
FIG 17

SRIVASTAVA, PRASAD, WAGNER

SiO$_2$ on n-type silicon
Temp 810 °C

FE/2.303 RT

-Log pO$_2$

Fig 18

Fig. 19

SRIVASTAVA, PRASAD, WAGNER

Legend (within figure):

□ Data of Mills and Kröger (11)
△ Data of Fused quartz (15)
○ Present work D.C. measurement
● Present work A.C. measurements (1 kH$_z$)
■ Present work A.C. data extrapolated to zero frequency

X-axis: $10^3/T$ °K
Y-axis: Log σ (ohm^{-1}cm^{-1})

FIG. 20

SRIVASTAVA, PRASAD, WAGNER.

Plot axes: y-axis "% Ionic conductivity" (0, 20, 40, 60, 80, 100); x-axis "T °C" (500, 600, 700, 800, 900, 1000). Legend: ● p-type, △ n-type.

END

FILMED

3-85

DTIC